Medicated multi-targeted alginate-based dressings for potential treatment of mixed bacterial-fungal infections in diabetic foot ulcers.

Asif Ahmed, Giulia Getti, Joshua Boateng*

School of Science, Faculty of Engineering and Science, University of Greenwich, Medway, Central Ave. Chatham Maritime, Kent ME4 4TB, UK.

* Correspondence: Dr Joshua Boateng (J.S.Boateng@gre.ac.uk; joshboat40@gmail.com)

Declarations of interest: None

Abstract

Recently developed medicated dressings target either bacterial or fungal infection only, which is not effective for the treatment of mixed infections common in diabetic foot ulcers (DFUs). This study aims to develop advanced bioactive alginate-based dressings (films and wafers) to deliver therapeutically relevant doses of ciprofloxacin (CIP) and fluconazole (FLU) to target mixed bacterial and fungal infections in DFUs. The alginate compatibility with the drugs was confirmed by SEM, XRD, FTIR and texture analysis, while the medicated wafers showed better fluid handling properties than the films in the presence of simulated wound fluid. The dressings showed initial fast release of FLU followed by sustained release of CIP which completely eradicated *E. coli*, *S. aureus*, *P. aeruginosa* and reduced fungal load (*C. albicans*) by 10-fold within 24 h. Moreover, the medicated dressings were biocompatible (> 70% cell viability over 72 h) with human primary adult keratinocytes and *in-vitro* scratch assay showed 65-68% wound closure within 7 days.

Keywords: Calcium alginate, ciprofloxacin, diabetic foot ulcer, dressing, fluconazole, mixed infection,

List of Abbreviations:

ATR-FTIR: Attenuated total reflectance Fourier transform infrared spectroscopy; **Aw**: Water absorption; **BLK**: blank; **CA**: Calcium alginate; **CIP**: Ciprofloxacin; **DFUs**: Diabetic foot ulcers; **DL:** Drug loaded; **EWC**: Equilibrium water content; **EWL**: Evaporative water loss; **GLY**: glycerol; **MTT:** Methylthiazolyldiphenyl-tetrazolium bromide; **PAF**: Peak adhesive force; **PEK**: Human primary epidermal keratinocytes; **SEM**: Scanning electron microscopy; **SWF**: simulated wound fluid; **WOA**: total work of adhesion; **WVTR**: Water vapour transmission rate; **XRD**: X-ray diffraction; **ZOI**: Zone of inhibition.

1. Introduction

Mixed bacterial-fungal (polymicrobial) infection is one of the most common complications of diabetic foot ulcers (DFUs). Bacteria and fungi work synergistically or antagonistically to promote survival of the species within a host-specific niche (Ahmed & Boateng, 2020; Dhamgaye et al., 2016). Patients with DFUs lack sensation (neuropathy) due to poor blood circulation in the foot area, which makes them unaware of deteriorating infections. The lack of treatment of wound fungal infection may lead to secondary bacterial infection resulting in a mixed infection and subsequently cause chronic foot ulceration, paronychias, cellulitis, gangrene, and osteomyelitis (Chadwick, 2013). Furthermore, the risk of amputations and mortality increases significantly with the onset of mixed bacterial and fungal infections. As shown by epidemiologic data, the occurrence of DFUs among diabetic patients is an average of 6.4% globally and 85% of amputations among patients with DFUs have been attributed to mixed infections (Zhang et al., 2017).

The prevalence of mixed infections in DFUs is a significant challenge in healing of chronic wounds. The interactions between bacteria and fungi in wounds is still ambiguous, but such interactions facilitate the biosynthesis of genes which alter the local wound environment to accelerate polymicrobial colonization leading to infection (Kalan & Grice, 2018). The most common mixed infections are caused by the interaction between *Candida albicans* (C. albicans) with either *Staphylococcus aureus* (*S. aureus*), *Pseudomonas aeruginosa* (*P. aeruginosa*) or *Escherichia coli* (*E. coli*) (Dhamgaye et al., 2016; Kalan & Grice, 2018). In this type of mixed infection, *C. albicans* activity initially compromises cell walls of the host cells, which facilitates the penetration of *S. aureus* into internal tissues. The *S. aureus* secretes proteases which help *C. albicans* to enhance its adhesion to the mucosal layer, resulting in synergistic growth of fungi (Nair et al., 2014). Moreover, *S. aureus* secretes coagulase that activates prothrombin, responsible for fibrin formation from fibrinogen. Formation of fibrin clots protect *C. albicans* from phagocytic killing by granulocytes (Nair et al., 2014). Untreated mixed infections in DFUs may lead to complex biofilm formation, which is associated with polymicrobial infections (Fourie et al., 2016).

Investigations of mixed infection in DFUs suggest that the treatment outcomes are very poor. Various studies have reported that several approaches such as cleansing followed by debridement, hyperbaric oxygen therapy, phage therapy and antimicrobial administration have been employed to prevent and control diabetic foot infections (Ahmed & Boateng, 2020; Peters et al., 2012). In the case of antimicrobial therapy, systemic administration (oral or parenteral) of high doses of antibiotics is prescribed to achieve adequate blood serum concentrations. The therapy recommended is 400 mg CIP parenterally three times a day or 500-700 mg CIP orally two times a day for moderate DFU infection. For severe infection, IV CIP 400 mg two times a day or oral CIP 500-750 mg two times a day along with other drugs such as metronidazole is recommended (Peterson *et al*., 1989). In a clinical study (Chellan *et al*., 2012), FLU combined with standard care for fungal infection in DFUs has been shown to be superior to standard care alone. In this study, 150 mg FLU tablet was given to the patients daily

and mild gastrointestinal symptoms were reported. The above IV / oral doses are associated with several side effects such as nausea and dizziness (Sanniyasi et al., 2015; Sarheed et al., 2016). In addition to that poor blood circulation at the lower extremities of diabetic patients makes oral and intravenous administered antibiotics ineffective (Sarheed et al., 2016). However, antimicrobial agents loaded into dressings have advantages of avoiding systemic side effects and can be delivered directly to the site of infected DFUs. Further, the local delivery of antimicrobial agents at lower doses is cheaper whilst significantly reducing the duration of treating infected DFUs which results in both health and economic benefits for patients and health care providers.

Current medicated modern dressings typically focus on the treatment of bacterial and fungal microbes separately, without considering the polymicrobial nature of chronic wounds such as DFUs. Metal based dressings such as silver and silver nanoparticles, copper, cobalt, nickel, ferric chloride, zinc oxide, gold and titanium showed promising results in eradicating bacterial load. However, there are not enough studies to establish their effectiveness against fungal infections (Anh et al., 2019; Mohandas et al., 2018). Further, these metal-based dressings have limitations due to their reported cytotoxicity (Paladini et al., 2014). Therefore, alginate-based biomaterials in the form of sodium or calcium alginate (CA) are used as advanced dressings for healing DFUs due to their biocompatible, adhesive, antibacterial and hemostatic properties (Hussain et al., 2017; Taskin et al., 2013). CA is rich in calcium ions which can be discharged into the wound bed from the dressings, caused by the interaction with sodium ions present in wound exudate resulting moist environment essential for effective wound healing (Cherng, 2020). Commercial alginate based dressings can be found as nonmedicated (only alginate or composite with other polymers) and medicated (with silver, honey, iodine, povidone and chlorhexidine) in the fom of hydrogels, hydrocolloids, foams, films and fibers (Aderibigbe & Buyana, 2018; Dumville et al., 2013). Recent studies showed that alginate based dressings incorporated with antibiotics (e.g., ciprofloxacin, gentamycin, silver sulphadiazine, strontium, streptomycin, vancomycin) or natural products (e.g., curcumin, essential oils, aloe vera), showed promise in reducing bacterial infections in DFUs (Aderibigbe & Buyana, 2018; Ahmas Raus et al., 2021; Ramirez-Acuna et al., 2019).

Ciprofloxacin (CIP) and fluconazole (FLU) are widely used as antibacterial and antifungal drugs to kill/inhibit causative bacteria (e.g. *E. coli*, *S. aureus*, *P. aeruginosa*) and *Candida* species present in DFUs respectively. A number of recent studies have been reported for CIP loaded dressings in the form nanofibers, nanogels, films, scaffolds and wafers for chronic wound application (Ahmed et al., 2018; Fan et al., 2021; Fang et al., 2020; Hashemikia et al., 2021; Sarwar et al., 2021). Recent studies have also been reported for FLU loaded dressings in the form of nanofibrous mats, hydrogels and natural rubber latex for fungal infections in wounds (Afrashi et al., 2021; Karthikeyan et al., 2015; Rewak-Soroczynska et al., 2021; Yonashiro Marcelino et al., 2018). However, treatment of mixed (bacterial/ fungal) infections in DFUs with a single medicated dressing containing both antibacterial (e.g. CIP) and

antifungal (e.g. FLU) remain under developed. This novel approch was reported in a recent study where a chitosan bandage was embedded with CIP and FLU loaded fibrin nanoparticles (Thattaruparambil Raveendran et al., 2019). That study established the proof of principle for simultaneous administration of both CIP and FLU within a single dressing for prolonged delivery. Though their study showed excellent potential for prolonged delivery of both CIP and FLU to treat mixed infections, the incorporation of drug loaded nanoparticles within dressing matrix while effective, presents a more complex system, that could potentially increase costs to patients and health services. A simpler matrix based dressing, that can release both drugs simultaneously in a sustained fashion over several days will have the advantage of therapeutically efficient but cost effective medicated dressing to treat mixed infections in DFUs. Therefore, the aim of this study was to formulate, and functionally characterize medicated CA based dressings in the form of films and lyophilized wafers containing broad-spectrum antibacterial (CIP) and antifungal (FLU) drugs to release both drugs in a controlled way to potentially target mixed infections in DFUs. In addition, the performance of the formulated medicated dressings (films and wafers) in terms of functional (fluid handling) and biological (antimicrobial, cell migration, and biocompatibility) properties was compared to a commercial hydrogel dressing (Actiformcool®). Actiformcool® was chosen in this study because it has been reported to have both antibacterial and fungal activity and it is prescribed for chronic ulcers (Moore, 2006). To the best of our knowledge this is the first study involving single wafer-based dressings loaded with both CIP and FLU for potential treatment of DFUs and compared with a commercial antimicrobial dressing. Wafer dressings are very easy to produce with high exudate handling activity (Ng, 2020) and has potential to provide a relatively cheap but therapeutically effective system for local delivery of both CIP and FLU to infected DFUs.

2. Materials and methods

2.1 Materials

Calcium alginate (CA) (mannuronate and guluronate ratio 59:41, molecular weight: 584.4 g/mol), ciprofloxacin (CIP), fluconazole (FLU), tris(hydroxymethyl)aminomethane, Mueller hinton broth, Brain heart infusion broth, Sabouraud dextrose broth**,** Dulbecco's phosphate buffered saline, trypsin-EDTA solution and foetal bovine serum were purchased from Sigma-Aldrich (Gillingham, UK). Sodium carbonate, sodium chloride, bovine serum albumin, hydrochloric acid, ethanol, acetic acid, acetonitrile, glycerol (GLY), Luria Bertani broth, streptomycin, agar (technical agar no. 3) and dimethyl sulfoxide were obtained from Fisher Scientific (Loughborough, UK). Calcium chloride was obtained from Riedel-de-Haen, Germany. HPLC vials were purchased from Chromatography, UK. Amphotericin B, a European pharmacopoeia reference standard was obtained from EDQM, Council of Europe. *E. coli* (ATCC 25922), *S. aureus* (ATCC 29213), *P. aeruginosa* (ATCC 27853) and *C. albicans* (ATCC 90028) were obtained from the microbiology lab of the University of Greenwich, UK.

Methylthiazolyldiphenyl-tetrazolium bromide (MTT) and trypan blue stain, 0.4% were obtained from Thermo Fisher Scientific (Paisley, UK).

2.2 Preparation of medicated films and wafers

2.2.1 Preparation of medicated films

To obtain films, GLY (33.33% w/w based on the total dry weight) was first dissolved in 0.014 M sodium carbonate solution by stirring at 50 ºC for 10 min. Then CIP and FLU were added (illustrated in Table 1) in the ratios of 1:10 (to obtain CIP and FLU concentration of 0.005% and 0.05% w/v respectively) and 1:20 (to obtain CIP and FLU concentration of 0.005% and 0.10% w/v respectively) to the hot solution with continuous stirring. After that, CA powder was added slowly to avoid lump formation with continuous stirring at 50 ºC for 3 h to obtain 1% w/v gels. Finally, 20 g of the resulting gels was poured into Petri dish (86 mm) and oven dried at 30 ºC for 18 h to obtain the films.

2.2.2 Preparation of medicated wafers

In the case of wafers, 1% w/v gels were prepared in the same way as for films but with no GLY and CIP and FLU were loaded accordingly (illustrated in Table 1) at the ratio of 1:10, 1:20 and 1:30 to achieve CIP concentration of 0.005% w/v and FLU concentration of 0.05%, 0.10 % and 0.15% w/v respectively. The lyophilized wafers were prepared by pouring the gels (1 g per well) into 24 well plates (diameter 15.6 mm) (Corning® Costar® cell culture plates; Sigma-Aldrich) and freeze-dried using a Virtis Advantage XL 70 freeze dryer (Biopharma Process Systems, Winchester, UK) in automatic mode with previously reported parameters (Ahmed et al., 2018).

Table 1. Quantities of polymer and drugs used during the preparation of gels for medicated films and wafers.

Formulation	CA (g)	GLY (g)	CIP (g)	FLU (g)	Total weight (g)
CA-BLK F	1.00	0.50	0.000	0.00	1.50
CA-CIP:FLU (1:10) F	1.00	0.50	0.005	0.05	1.56
CA-CIP:FLU (1:20) F	1.00	0.50	0.005	0.10	1.61
CA-BLK W	1.00	0.00	0.000	0.00	1.00
CA-CIP:FLU (1:10) W	1.00	0.00	0.005	0.05	1.06
CA-CIP:FLU (1:20) W	1.00	0.00	0.005	0.10	1.11
CA-CIP:FLU (1:30) W	1.00	0.00	0.005	0.15	1.16

*Quantities reported were for 100 ml of the solvent (0.014 M sodium carbonate)

2.3 Physico-chemical characterization

2.3.1 Scanning electron microscopy (SEM)

Morphological and microscopic analysis of films and wafers was carried out with a Hitachi SU 8030 (Hitachi High-Technologies, Germany) scanning electron microscope, operated at 10 KV and working

distance of 8.1 mm for films and 21.4 mm for wafers. All the samples were sputter-coated using either chromium or gold and the images were taken at magnifications of x200 and x6000 using i-scan 200 software.

2.3.2 X-ray diffraction (XRD)

The X-ray diffraction patterns of the starting materials and the formulated dressings were analysed by a D8 Advance X-ray diffractometer (Bruker, Germany) in transmission mode. The X-ray source was operated at a voltage and current of 40 KV and 40 mA respectively. The samples were scanned in the 2-theta range of 5-50º with a step size of 0.02º/s at a rotation speed of 15 rpm.

2.3.3 Attenuated total reflectance Fourier transform infrared spectroscopy (ATR-FTIR)

A Spectrum Two Perkin Elmer spectrophotometer (Perkin Elmer, USA) equipped with a crystal diamond universal attenuated total reflectance was used to identify the characteristic functional groups in the starting materials (polymer and drugs) and their incorporation into the dressing matrix. The FTIR spectra of all samples were collected within a range of 650-4000 cm^{-1} at a resolution of 4 cm^{-1}.

2.3.4 Mechanical properties

The tensile properties (tensile strength, Young's modulus and percent elongation at break) of the films and hardness of freeze-dried wafers were measured at room temperature using a TA HD Texture analyser (Stable Microsystem Ltd., Surrey, UK) fitted with a 5 kg load cell. The data were plotted and displayed using *Texture Exponent 32* software program. The films (n = 3), were cut in the shape of a dumbbell (30 mm gauge length and 3.5 mm width) and stretched between two tensile grips at a cross head speed of 0.10 mm/sec with a trigger force 0.05 N. The hardness of wafers was measured by compressing each wafer at three different locations in compression mode using the following settings: 0.001 N trigger force, 2 mm depth of penetration, 1 mm/sec test speed and 10 mm return distance.

2.3.5 Adhesive properties

Set gelatine gel (6.67% w/w) with 0.5 ml of simulated wound fluid (SWF) evenly spread over the surface, was used as representative chronic wound surface. The SWF comprised 2% (w/w) bovine serum albumin, 0.02 M calcium chloride, 0.4 M sodium chloride and 0.08 M tris (hydroxymethyl) aminomethane in deionized water. Prior to testing, the samples were attached to a cylindrical stainless-steel probe (35 mm diameter) with the help of double-sided adhesive tape. The dressing fitted onto the probe was lowered until it made contact with the surface of the gelatine gel. The texture analyser was set to run in tensile mode; followed by 60 s contact time with applied force of 1 N and detached at pre-test and test speeds of 0.5 mm/s and post-test speed of 1 mm/s, 0.05 N trigger force and 10 mm return distance. The maximum force required to separate dressings from the surface of gelatine gel, the area under the curve of force versus distance plot and the total distance (in mm) travelled by dressings till

complete separation were recorded to represent stickiness or peak adhesive force (PAF), total work of adhesion (WOA) and cohesiveness respectively. Each formulation was tested in triplicate (n = 3).

2.3.6 Porosity

The porosity of the films, wafers and commercial product (Actiformcool®) was measured using a liquid (ethanol) displacement method (Catanzano et al., 2017). The films and Actiformcool® were cut into circular disks to achieve similar diameter as the wafers and the diameter and thickness of the samples were measured by a digital Vernier calliper electronic micrometre gauge to calculate the total pore volume (V_0). The samples were weighed (W_0) and then immersed in 10 ml of ethanol for 3 h to achieve saturation. The excess liquid was blotted with tissue paper and the sample quickly weighed (W_1) on an analytical balance (n = 3). The porosity of the dressings was calculated using Eq. (1).

$$Porosity\ (\%) = (W_1\text{-}W_0)/(\rho_{eth}V_0)\ x\ 100 \quad (1)$$

ρ_{eth} *: density of ethanol = 0.789 g/cm*^{3}

2.4 Fluid handling properties

2.4.1 Water absorption (Aw), equilibrium water content (EWC) and swelling index

A SWF pH of 7.5 was used to mimic chronic wound exudate. The samples were initially weighed and then immersed in 10 ml of SWF at 37 ºC in an incubator for 24 h for Aw and EWC tests. After that, the swollen samples were carefully lifted and excess water on the surface removed before measuring the final (swollen) weight. The Aw and EWC (n = 3) were calculated using Eqs. (2-3) below.

$$Aw(\%) = \frac{Ws-Wi}{Wi} x\ 100 \quad (2)$$

$$EWC(\%) = \frac{Ws-Wi}{Ws} x\ 100 \quad (3)$$

Where Ws is the swollen weight and Wi is the initial weight before immersion into SWF.

For swelling index, the swollen weights of the dressings were recorded at specific time intervals after taking initial dry weight. The swelling index was calculated (n = 3) from Eq. (4) below.

$$Swelling\ index\ (\%) = \frac{Wst-Wi}{Wi}\ x\ 100 \quad (4)$$

Where W_i is the dry weight of samples before hydration and W_{st} is the swollen weight of samples at different hydration times. Each measurement was performed in triplicate (n = 3)

2.4.2 Water vapour transmission rate (WVTR)

The capability of moisture permeability was determined by measuring WVTR of the formulated alginate dressings and the commercial hydrogel, (Actiformcool®). The dressings were mounted on top of open cylindrical plastic tubes (15 mm diameter) containing 4 ml of deionized water with 8 mm air gap between the samples and water surface and sealed with epoxy glue across the edges to prevent any water vapour loss around the edges. The set up was then kept in an air-circulated oven for 24 h at 37 °C and the WVTR was calculated using Eq. (5).

$$WVTR = \frac{Wi-Wt}{A} x10^{6}\, g/m^{2}\, day^{-1} \quad (5)$$

Where A is the area of the mouth of the plastic tube (πr^2), Wi and Wt are the weight of the whole setup before and after placing into the oven, respectively.

2.4.3 Evaporative water loss (EWL)

The EWL was determined by immersing the samples in 10 ml of SWF for 24 h in an oven (37 °C). The resulting samples were weighed at regular time intervals until steady state and the EWL estimated with Eq. (6)

$$Water\ loss\ (\%) = W_t/W_o\ x\ 100 \quad (6)$$

Where W_t and W_o represent the weight after time 't' and initial weight, respectively.

2.4.4 Moisture content

To measure residual moisture content of the dressings, thermogravimetric analysis (TGA) was performed using a Q5000-IR TGA instrument (TA Instruments, Crawley, UK). About 1.0 - 1.5 mg of sample was loaded into an aluminium pan and heated from ambient temperature (~25 ºC) to 300 ºC at 10 ºC/min under inert nitrogen gas at a flow rate of 50 ml/min. The measure of water content was determined by weight loss at 100 ºC using *TA Instruments Universal Analysis 2000* software program.

2.5 In-vitro drug dissolution and release profiles

Drug dissolution of the formulated dressings was carried out using diffusion cell method developed in house at the University of Greenwich as previously reported (Catanzano et al., 2017). A SWF (pH 7.5) without BSA (to avoid blocking HPLC column) was used as dissolution medium and maintained at 37 °C with constant magnetic stirring (600 rpm). Aliquots (1 ml) of the dissolution medium (n = 3) were collected at specific time points from the diffusion cell, analysed by HPLC and the drug release profiles (% drug release vs time) plotted. The sampled aliquots were always replaced with dissolution media at the same temperature.

2.5.1 HPLC analysis

The dissolution media sampled and drug content uniformity within each formulated dressing (Table S2 and Fig. S2) were analysed using a HPLC system (Agilent 1200 series, Agilent Technologies, UK) with a C18 analytical column (YMC-Pack ODS-AQ AQ-303-5, 250 x 4.6 mm I.D, S-5 µm, 120A, NO.042512322). A two-solvent (2% acetic acid and acetonitrile) mobile phase in isocratic elution mode was used for the separation of CIP and FLU at room temperature at a flow rate of 1 ml/min, injection volume of 20 µl and detector wavelength of 264 nm. The calibration standard curves for CIP and FLU were acquired over a range of 1-100 µg/ml and 25 - 500 µg/ml respectively.

2.6 Antibacterial and antifungal (mixed infections) study

In vitro mixed infections study of the formulated medicated dressings and Actiformcool® was carried out by turbidimetric and *Kirby Bauer* disk diffusion assays. The following mixed cultures were obtained in brain heart infusion (BHI) broth medium at 37 ºC: *C. albicans* and either *E. coli* (*i.e., C. albicans + E. coli*), *P. aeruginosa* (i.e., *C. albicans + P. aeruginosa*) or *S. aureus* (i.e. *C. albicans + S. aureus*). Minimum inhibitory concentrations (MIC) for CIP and FLU and minimum fungicidal concentrations (MFC) for FLU were also determined (see supplementary data – Fig. S3 and Fig. S4)

2.6.1 Turbidimetric assay

In the turbidimetric assay, the formulated drug loaded (DL) dressings and Actiformcool® were placed in 10 ml of BHI broth containing both bacteria (10^6 CFU/ml) and fungi (10^5 CFU/ml) to represent mixed infections chronic wound. Control tubes contained either *C. albicans* alone, bacteria alone or medium alone. The absorbance was measured at 540 nm using a micro-plate reader at different time intervals (3, 6, 24, 48, and 72 h). CFU assay was also performed in which 0.1 ml aliquots were taken, serially diluted with Ringer's solution, and plated on Luria Bertani agar. The Luria Bertani agar was supplemented with amphotericin B at a concentration of 25 µg/ml to prevent non-targeted fungal growth and Sabouraud dextrose agar was supplemented with streptomycin at a concentration of 40 µg/ml to prevent non-targeted bacterial growth. The Sabouraud dextrose agar and Luria Bertani agar plates were incubated at 30 ºC and 37 ºC respectively and the bacterial and fungal cells were counted after 24 h.

2.6.2 Kirby Bauer disk diffusion assay

In the *Kirby Bauer* disk diffusion assay, the mixed infections were formed by taking 0.1 ml of bacterial suspension (10^8 CFU/ml) and 1 ml of fungal suspension (10^6 CFU/ml) from the prepared inocula and mixed in 8.9 ml of BHI broth. This resulted in final concentrations of 10^6 CFU/ml for bacteria (*E. coli*, *P. aeruginosa* and *S. aureus*) and 10^5 CFU/ml for fungi (*C. albicans*). The mixed suspensions were streaked onto the BHI agar plates with the help of a sterile swab. The combined medicated film (6 mm diameter) and wafer (14.5 ± 0.5 mm diameter) were placed onto the inoculated agar surface and incubated at 37 ºC for 24 h, control plates were incubated without dressing.

Experiments were carried out in triplicates and the growth inhibition zones measured using a Vernier calliper. Images of zone of inhibition (ZOI) were taken as supplementary information. ZOI assay of Actiformcool® was not performed due to its highly sticky nature.

2.7 MTT (cell viability) assay

Cell viability (proliferation) was determined by an indirect cytotoxicity assay in which sample extracts were tested instead of direct contact of dressings with the cells. The samples were extracted according to previously reported procedure (Ahmed et al., 2018). In brief, the dressings were first sterilized with UV radiation and dipped into 2.5 ml of dermal basal cell medium (PCS-200-030, ATCC) supplemented with growth kit (PCS-200-040, ATCC) for 24 h of incubation at 37 ºC in Heracell 150i CO_2 incubator (Thermo Scientific). After incubation, the sample extracts were collected through filtration using 0.2- µm filter. In this study, the formulated dressings and Actiformcool® were tested on human primary epidermal keratinocyte (PEK) cells (PCS-200-011, ATCC). The cells were cultured in dermal basal cell medium and seeded into 96-well tissue culture plates at a density of 10^4 cells/well. After 5 h incubation at 37 ºC in 5% (*v/ v*) CO_2, when the cells had attached onto the bottom surface of the plates, the media was replaced with sample extracts ($n = 3$) and the cells were further incubated for up to 72 h. The viability of cells cultured with sample extracts was determined at 24, 48 and 72 h. The absorbance of the solutions was measured at 492 nm by a microtiter plate reader (Multiskan FC, Thermo scientific) equipped with SkanIt for Multiskan FC 3.1 software (Thermo scientific). The viability of cells cultured with Triton-X-100 (0.01 w/v) and with fresh media was considered as positive and negative controls respectively whilst Actiformcool® was used as a representative standard commercial sample. Every experiment was carried in three biological replicates. The percentage cell viability was calculated from Eq. (7).

$$Cell\ viability\ (\%) = \frac{At-Ab}{Ac-Ab} * 100 \quad (7)$$

Where *At*, *Ab* and *Ac* are the absorbance of tested samples, medium only and negative control (untreated cells) respectively. In addition, after each time point (24, 48 and 72 h), the morphology of the cells was captured with a fluorescence microscope (Nikon Eclipse Ti-U, UK).

2.8 In vitro wound scratch (cell migration) assay

The PEK cells were seeded into 24-well tissue culture plates at an initial density of $5x10^4$ cells/well so that they could reach about 80–85% confluence as a monolayer after overnight incubation. However, if the cell layer did not achieve this confluence, the incubation period was extended until confluency was reached. A wound gap was created with a sterile 200 µl micropipette tip by scratching in the monolayer vertically (Satish & Korrapati, 2015). To create a consistent gap size, scratching was performed at the centre of each well with the same size of micropipette tip. The gap distance was equal to the outer diameter (775 µm) of the end of the tip. After scratching, the wells were gently washed

twice with Dulbecco's phosphate buffered saline without affecting the monolayer to remove the detached cells. The extracts of selected formulations (CA-BLK F, CA-CIP: FLU (1:10) F, CA-BLK W and CA-CIP: FLU (1:10) W) were then added to each well. Wells treated with Triton-X-100 (0.01% w/v) and untreated wells were considered as negative and positive controls respectively. In addition, Actiformcool® was chosen as representative standard commercial sample to validate the experiment. The migration of cells (representing wound closure) was observed by a fluorescence microscope (Nikon Eclipse Ti-U, UK) and digital images were captured at time intervals of 0, 1, 2, 3, 7, 8 and 9 days in green bright field mode. To obtain the maximum field of view, a low magnification (4x objective lens) was also used whilst capturing images and the wound gaps were evaluated using NIS-Elements software. The percentage of wound closure was calculated based on the length (µm) of wound measured at the specific time as shown in Eq. (8) (Amin et al., 2017).

$$Wound\ closure\ (\%) = \frac{d_0 - d_t}{d_0} \quad (8)$$

Here, d_0 represents the length (µm) of the wound was initially created, and d_t refers to the length (µm) of the wound recorded at specific time intervals.

2.9 Statistical analysis

The statistical differences in the results were evaluated by Student *t-test* and *ANOVA*. Differences with a *p* value of 0.05 or less was statistically significant. The results are presented as mean of 3 replicates (± standard deviation).

3. Results and discussion

3.1 Formulation of medicated film and wafer dressings

Drug precipitation or uncontrolled recrystallization of drug is the most noticeable problem in formulating solvent cast films especially when loaded with high concentration of drugs resulting in a rough surface (Centkowska et al., 2020). However, the formulated DL films appeared to be translucent with no precipitated drugs visible on the surface while wafers were not transparent compared to the films. Transparency depends on the passing of light through the matrix and in the case of wafers, light scatters outward incoherently and does not pass through to a noticeable extent due to the interconnected pores throughout its matrix. However, all wafers appeared to be of uniform texture and thickness. Moreover, there was no visible drug precipitation on the surface of the wafers indicating drug distribution throughout the porous matrix which was also confirmed by drug content uniformity (Table S3).

3.2 Physico-chemical characterization

3.2.1 Scanning electron microscopy (SEM)

The solvent cast films appeared as continuous sheets. As shown in Fig. 1, spherulitic crystallization was observed in DL films whereas the BLK film (no drug) appeared as rough surface due to presence of $CaCO_3$ (confirmed by XRD, Fig. 2B). The addition of FLU and CIP into the polymer matrix suppressed the polymer chain mobility resulting in spherulitic crystallization (Hsu & Yao, 2014) this might explain the fibrillar morphology observed for the CA-CIP:FLU films. The crystalline nature of the drugs was also confirmed by XRD (Fig. 2A). Furthermore, all the films showed complete absence of any porous structure, which implies that all the components were homogeneously dispersed in the matrix during drying, resulting in a continuous sheet of polymeric films. The lyophilized wafers showed porous matrix with wafers containing CIP and FLU in the ratios of 1:10 and 1:20 retaining large circular and uniform pore size distributions as shown in Fig. 1. Wafers incorporated with CIP and FLU in the ratio of 1: 30 showed non-uniform pores with reduced pore size. This could be attributed to the higher content of FLU in the wafer's matrix resulting in denser pores.

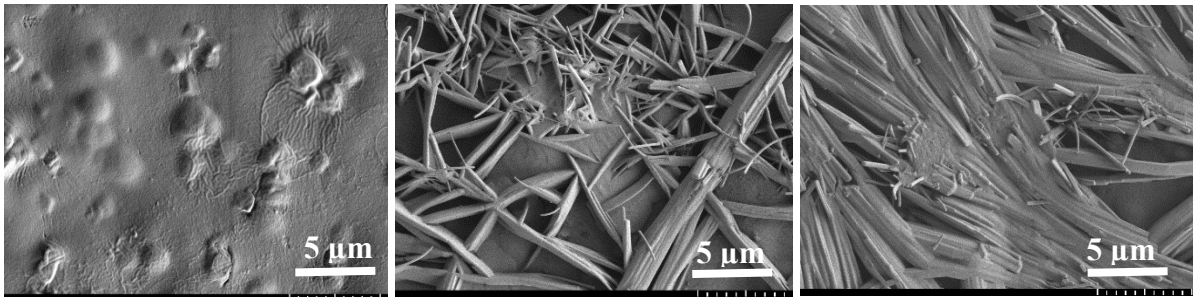

CA-BLK F **CA-CIP:FLU (1:10) F** **CA-CIP:FLU (1:20) F**

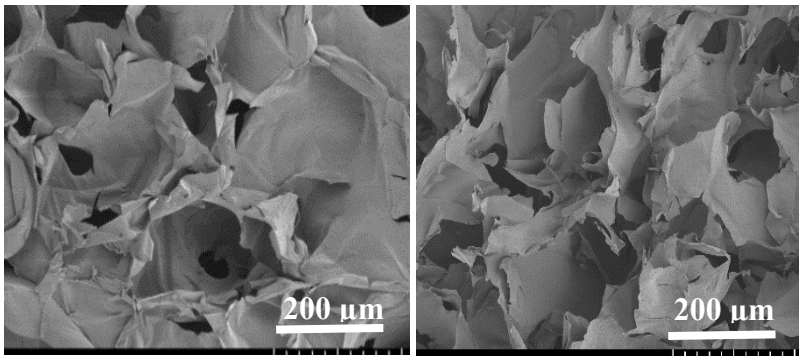

CA-BLK W **CA-CIP:FLU (1:10) W**

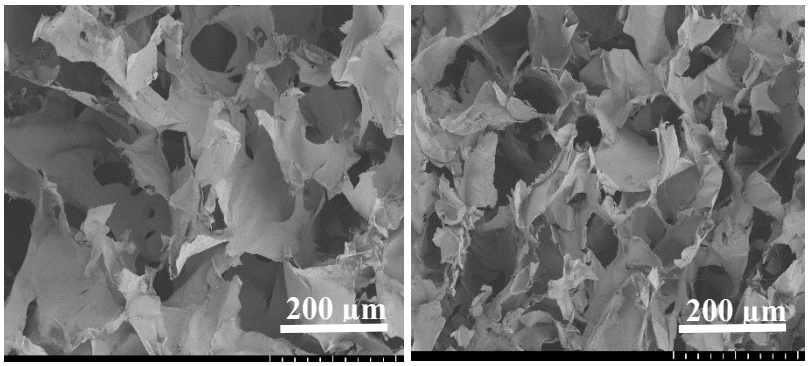

CA-CIP:FLU (1:20) W **CA-CIP:FLU (1:30) W**

Fig. 1. Surface morphology of the formulated film and wafer dressings. The SEM micrographs of films and wafers were captured at magnifications of x6000 and x200 respectively. F: Film and W: Wafer

3.2.2 X-ray diffraction (XRD)

The XRD diffractogram of pure CIP showed three distinct sharp peaks at 14.43º, 20.67º and 25.50º while FLU exhibited several characteristic sharp peaks at 2θ of 9.16º, 15.09º, 16.14º and 20.03º (Fig. 2A). The physical mixture of FLU and CIP mainly showed the peaks identical to pure FLU, which could be due to significantly higher amounts of FLU present compared to CIP. In the XRD diffractograms of formulated dressings, eight common peaks (at 2θ of 22.81º, 29.58º, 31.76º, 36.07º, 39.42º, 43.16º, 47.64º and 48.5º) appeared in all BLK and DL formulations (Fig. 2B) and were matched with the peaks of $CaCO_3$ (Ahmed & Boateng, 2018). The distinct peaks of CIP at 2θ of 14.43º, 20.67º and 25.50º were not observed in the DL films meaning CIP was molecularly dispersed into the film matrix.

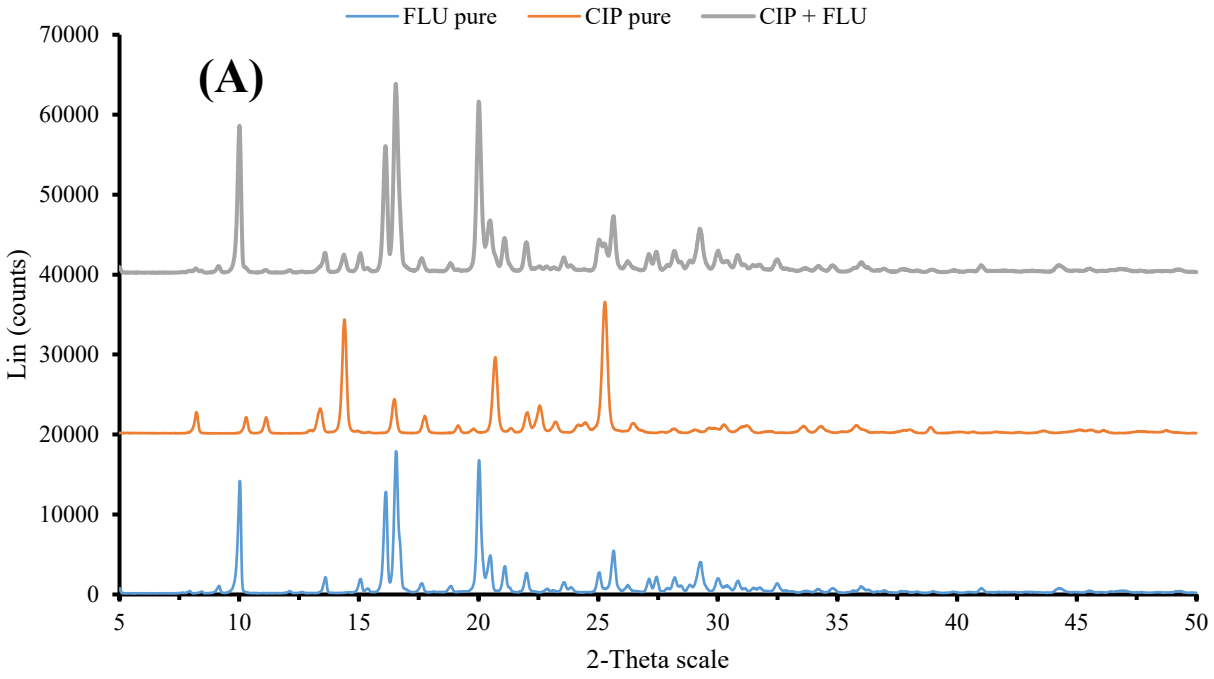

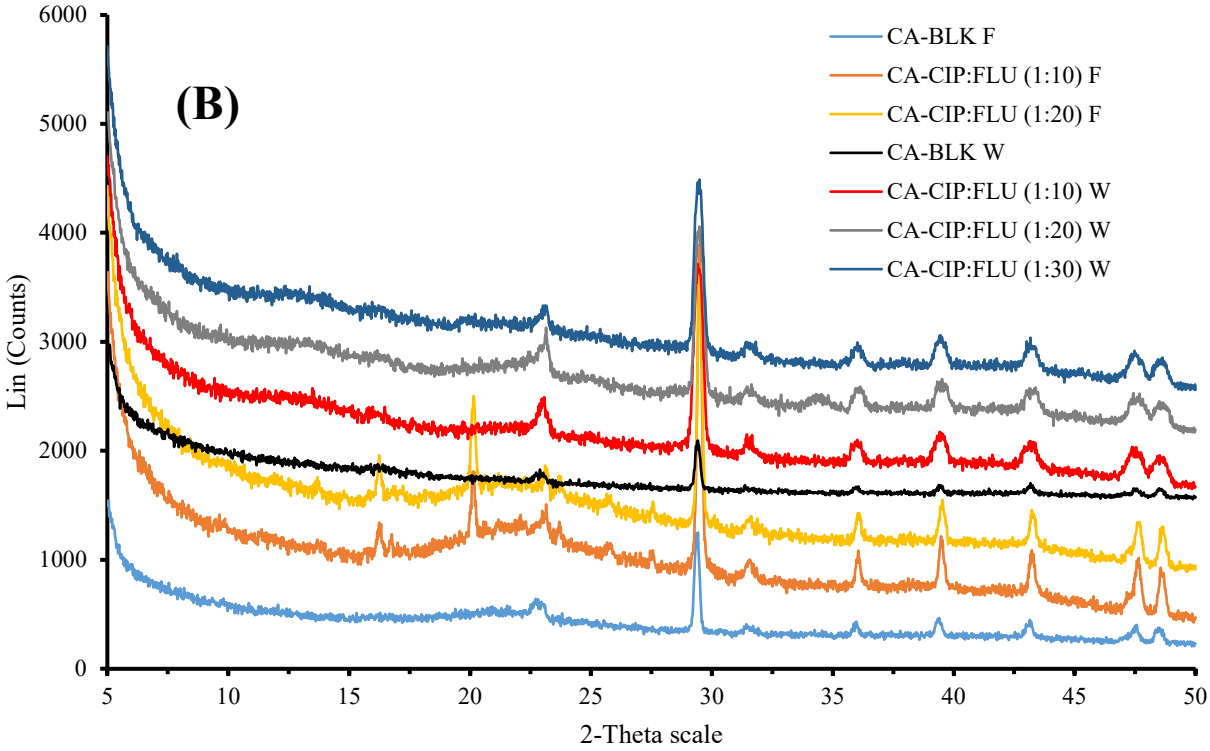

Fig. 2. X-ray diffractograms of (A) pure FLU, pure CIP and physical mixture of FLU+CIP and (B) DL film (F) and wafer (W) dressings.

However, the two sharp peaks of FLU at 2θ of 16.14º and 20.03º (Fig. 2A) appeared in the diffractograms of DL films indicating only partial molecular dispersion of the drug within the film matrix. This was attributed to the higher amount of FLU loaded initially, compared to CIP as well as its lower water solubility, which had impact on the film sheets. No peaks of CIP and FLU appeared in the diffractogram of DL wafers compared to BLK wafers, implying that the lyophilisation process induced better drug molecular distribution throughout the matrix, which corroborated with SEM observations. Therefore both the films and wafers appeared as crystalline in nature due to presence of $CaCO_3$. The crystallinity of CaCO3 was lower in films than wafers due to the presence of plasticizer (GLY) in the film dressings which could mask the crystalline $CaCO_3$ precipitates.

3.2.3 Attenuated total reflectance Fourier transform infrared spectroscopy (ATR-FTIR)

The FTIR analysis was carried out to determine the compatibility and possible chemical interaction between the drugs and alginate within the formulated dressings. The FTIR spectra of all DL wafers and films containing CIP and FLU in the ratio of 1:10 were identical to that of the BLK wafers and films (Fig. 3). This indicated that both drugs at low doses were homogeneously distributed throughout the dressing matrix which was in good agreement with visual observation and confirms the compatibility between the drugs and polymer within the dressings. The characteristic peaks of CIP, FLU and CA are tabulated in Table S4 (supplementary information). The characteristic peaks of CIP (aryl fluoride at 1050 cm^{-1}, carbonyl group at 1450 cm^{-1} and quinolones at 1650 cm^{-1}) and FLU (C=C

stretching of 2,4-difluorobenzyl group at 1618 cm^{-1}, C-H_2 scissor of propane backbone at 1408 cm^{-1}, CH deformation of 2,4-difluorobenzyl group at 1075 cm^{-1} and C-(OH) stretching of propane backbone at 1011 cm^{-1}), were not observed in the spectra of DL CIP:FLU 1:10 wafers and films. This could be due to relative similarity and shifting of the peaks due to the secondary interactions (i.e., hydrogen bonding and van der Waals) of drugs with the polymer. This also suggests the possible molecular dispersion of drug within the polymeric matrix. However, most of the FLU peaks were seen in the spectrum of the film containing CIP and FLU in the ratio of 1:20 (Fig. 3). This could be because once the saturation point of molecular dispersion is reached, excess FLU crystalizes out of the polymer matrix during drying and subsequent film formation. In the FTIR spectra, the OH stretching of CA appeared as a broad peak (3638 – 2941 cm^{-1}) and CIP (3600 – 3045 cm^{-1}) but was a narrow peak for FLU (3715 – 3633 cm^{-1}) (Table S1). This clearly suggests that the CA has higher hydrogen bonding affinity with CIP than with FLU.

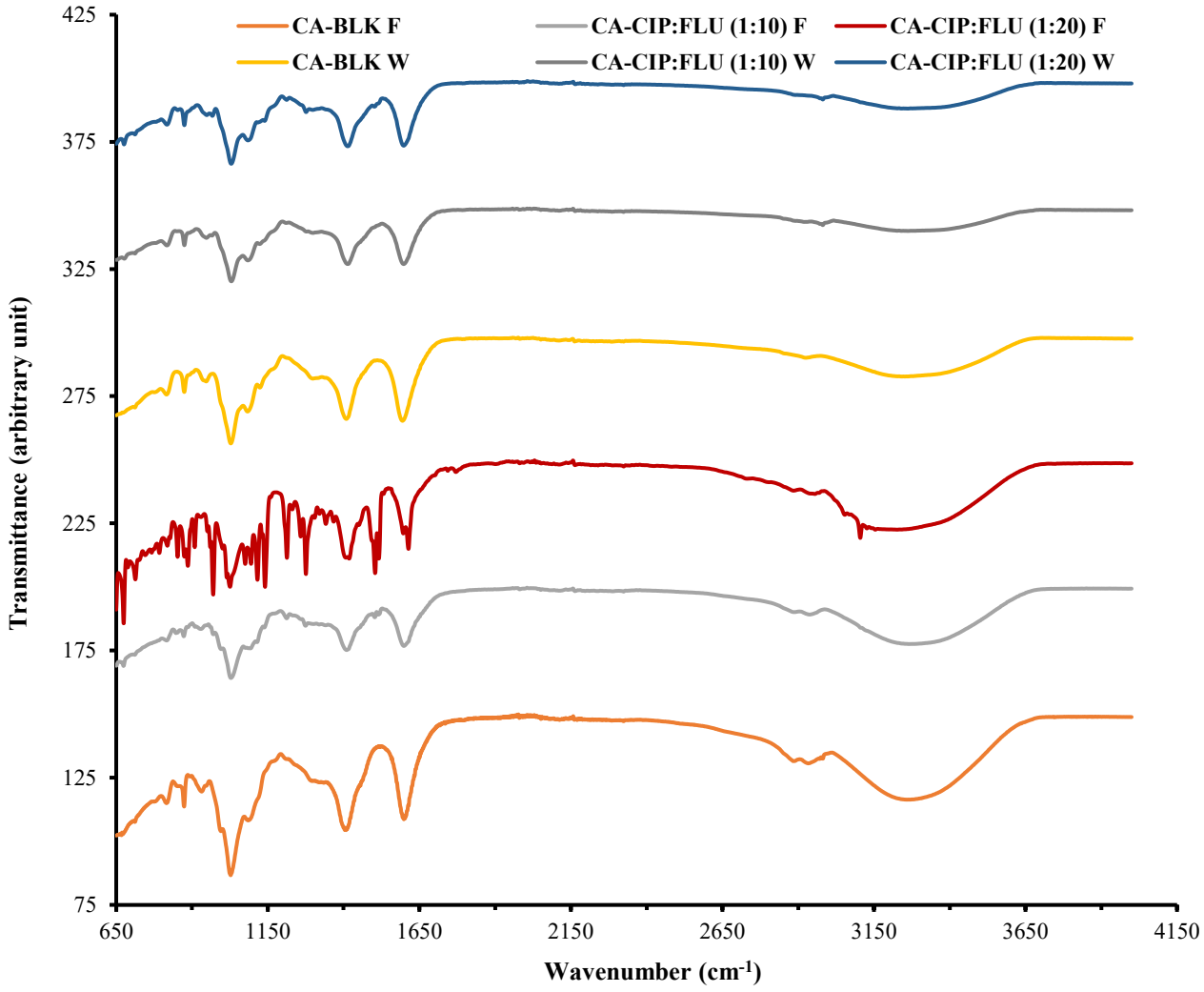

Fig. 3. FTIR spectra of BLK and DL dressings (films and wafers).

3.2.4 Mechanical properties of films and wafers

Adequate mechanical strength is required for physical stability during handling as well as avoiding potential contact irritation during application (Rezvanian et al., 2016). As shown in Fig. 4A, there were no statistically significant difference in tensile strength ($p > 0.05$), Young's modulus ($p > 0.05$) and percent elongation ($p > 0.05$) between the BLK and DL films. This indicates that addition of drugs had no impact on the mechanical characteristics of the films. The tensile strength and rigidity (Young's modulus) of the films were optimum, easy to handle, durable and stress resistant. However, the formulated films did not show ideal values (30-50%) of elasticity (Boateng & Popescu, 2016), but they were still easy to handle without breaking. The ratio of guluronic and mannuronic acid side chains as well as the source and extraction of alginate play vital roles in tensile properties of CA films (Gao et al., 2017). The elasticity of the formulated films can be further improved by combining with other synthetic and natural polymers (Pawar et al., 2013).

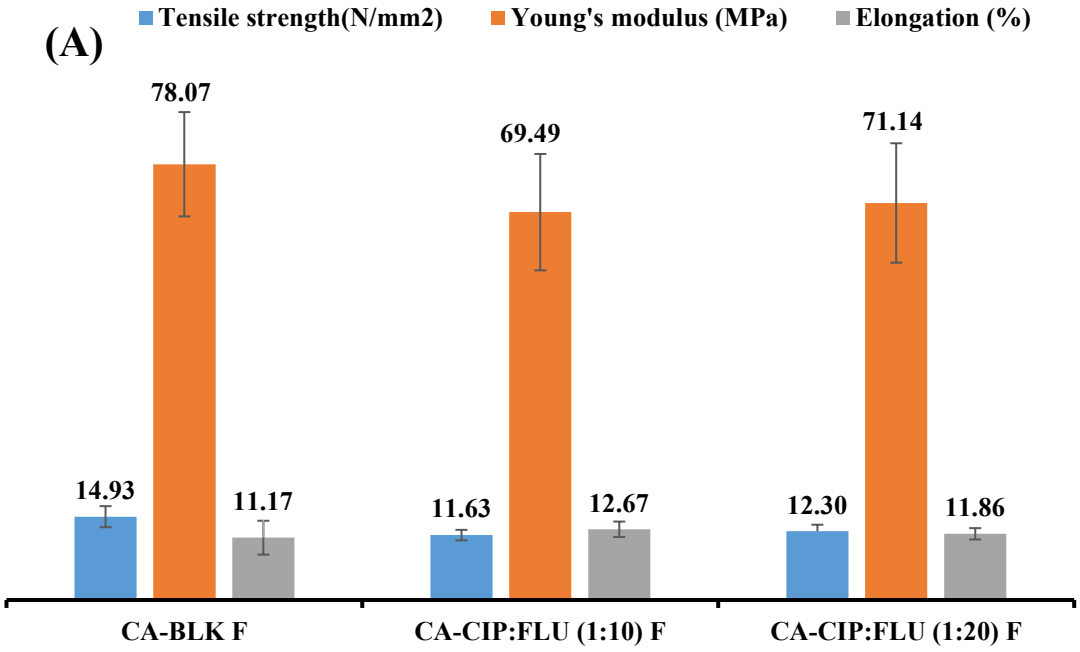

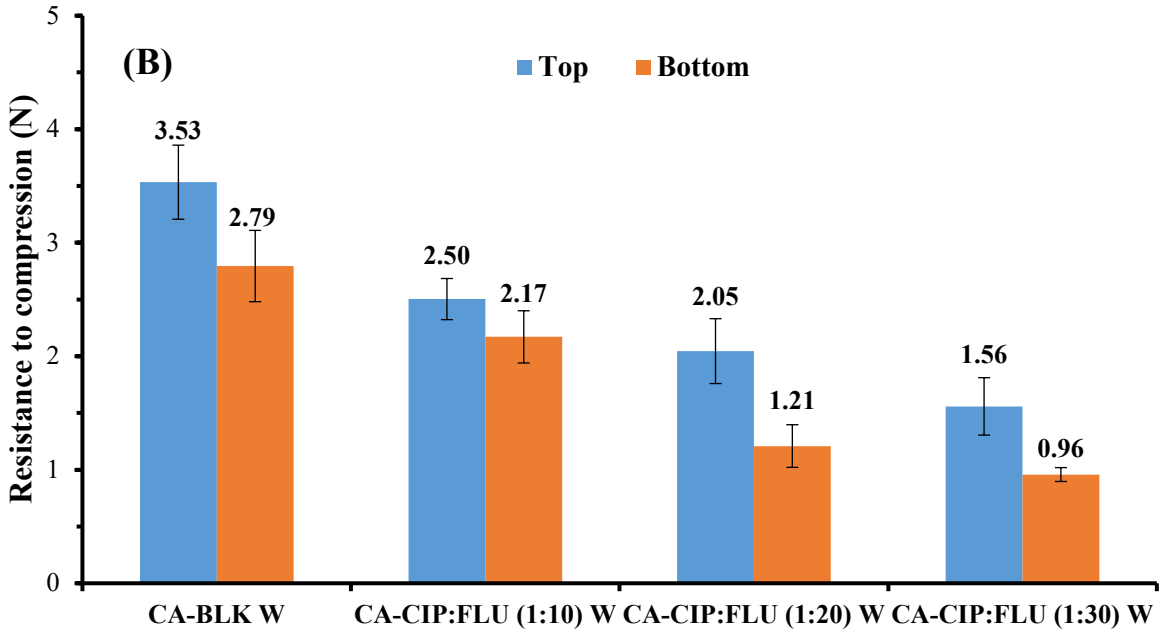

Fig. 4. Mechanical properties of BLK and DL films (a) and wafers (b)

DL wafers showed hardness values (Fig. 4B) of the top side between 2.50 ± 0.18 and 1.56 ± 0.25 N and about 2.17 ± 0.23 to 0.96 ± 0.06 N at the bottom which were significantly lower ($p < 0.05$) lower compared to BLK wafers (top: 3.53 ± 0.33 N and bottom: 2.79 ± 0.31 N). This could be because incorporation of drugs enhanced the hydrogen bonding between the drug and CA molecules which subsequently reduced the intermolecular interactions between the polymer chains. This enhanced the mobility of CA molecular chains with resultant decrease in rigidity of the wafers. Wafers containing CIP and FLU in the ratio of 1:10 showed the highest hardness (about 2.50 ± 0.18 N) compared to the other DL wafers. This could be because this formulation exhibited uniform pore size distribution (confirmed by SEM observation, Fig. 1) resulting in higher resistance to compressive deformation. It was also observed that the hardness of DL wafers decreased with increasing amount of FLU. This could be explained by the fact that the addition of high amounts of FLU might cause loss of structural integrity of the wafers which subsequently suppressed the rigidity of the polymeric matrix. It can also be seen from Fig. 4B that the hardness on the lower side of the wafers was slightly (but not significant $p > 0.05$) lower than the top side. One reason for this phenomenon is that the lower part of the wafers had lower polymer density causing a looser structure. This is common in shelf type freeze dryers used in this study, where freezing starts from the bottom of the gel upwards due to condenser being below the sample within the instrument chamber.

3.2.5 Adhesive properties

DL films showed significantly ($p < 0.05$) lower stickiness (0.76 ± 0.04 N, and 0.63 ± 0.13N) and WOA (0.44 ± 0.08 N.mm and 0.63 ± 0.13 N.mm) compared to BLK films (2.21 ± 0.31 N & 1.47 ±

0.31 N.mm). This could be because once the DL films got hydrated with SWF, FLU precipitated on the surface of the films resulting in reduced plasticizing effect, which ultimately decreased stickiness. The DL films exhibited significantly ($p < 0.05$) higher cohesiveness than BLK film (Fig. 5) indicating that the medicated films will adhere onto the wound surface better than the film without drug.

The PAF values of DL wafers were significantly ($p < 0.05$) lower than BLK wafers (Fig. 5) due to incorporation of drugs which enhanced the hydrogen bonding between the drug and CA molecules resulting in higher content of bound water than BLK wafers (confirmed by TGA analysis). Therefore, the hydration capacity of DL wafers on the model wound surface (gelatine gel) was reduced in the presence of SWF resulting in lower stickiness than the BLK wafers. In addition, the pore size distribution of wafers within the matrix was affected after drug loading resulting in further reduction in the hardness and consequently lower stickiness than the BLK wafer. Wafers containing CIP and FLU in the ratios of 1:10 and 1:20 showed higher cohesiveness values at 3.77 ± 0.18 and 4.03 ± 0.41 mm respectively than the corresponding BLK wafers (2.00 ± 0.42 nm). The wafers containing CIP and FLU in the ratio of 1:30 exhibited cohesiveness of 1.94 ± 0.47 nm which was similar to the BLK wafer.

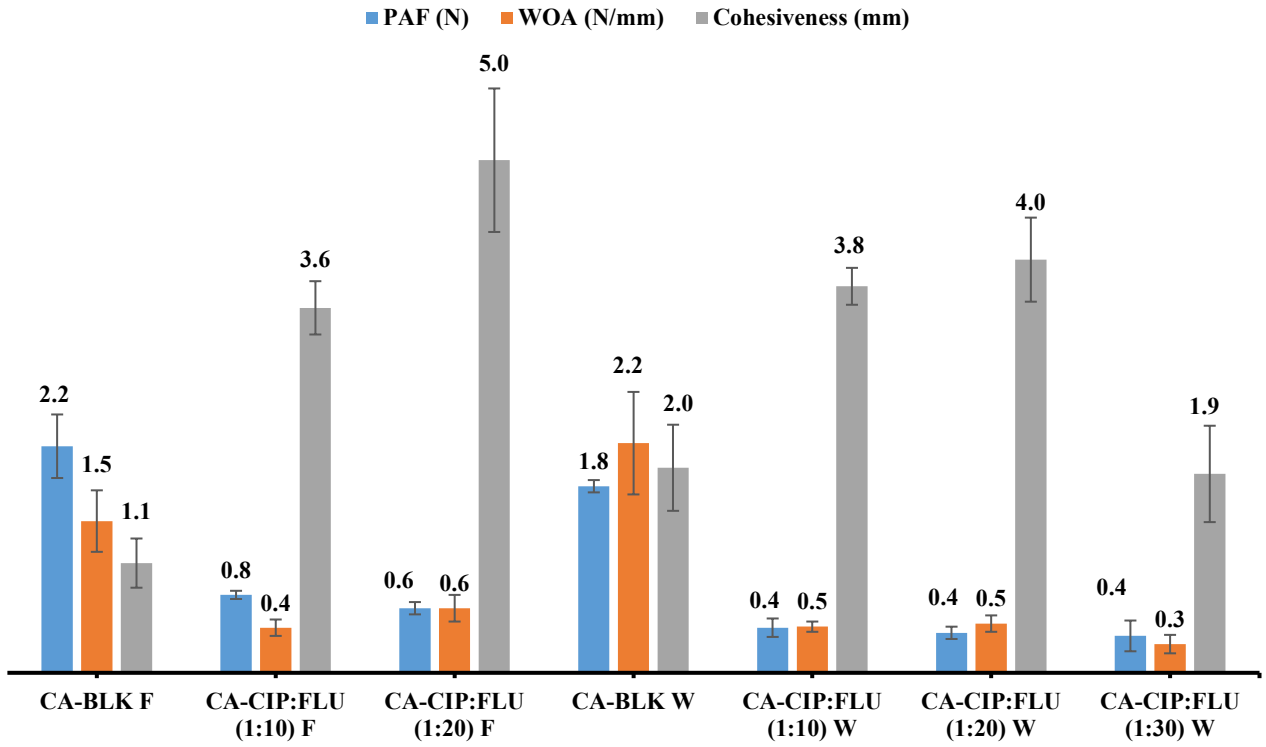

Fig. 5. *In vitro* adhesive properties of BLK and DL films (a) and wafers (b)

3.2.6 Porosity

Porosity of dressings plays an important role in rapidly absorbing exudates from the chronic wound beds. The wafer dressings were observed as highly porous whereas film dressings appeared as continuous sheets with minimal porosity. The porous structure of the wafers was acquired by lyophilisation technique in which the frozen gels are sublimed from its frozen state under vacuum at

low temperature, leaving a microporous structure within the polymeric matrix (Ng, 2020). According to Table 2, DL films showed higher porosity (42.34−44.43%) than BLK film (38.34 ± 3.80%). This could be explained by the fact that loading of drugs into the film sheets reduced the intermolecular polymer chain interaction that enhanced void space in the polymeric matrix followed by decreasing rigidity (Fig. 4A). It was also observed that the films containing high amount of FLU (CA-CIP: FLU 1:20) showed lower porosity than the CA-CIP:FLU 1:10 film because, FLU had the tendency to increase intermolecular interaction resulting in decreased mobility and therefore, tighter spaces between the polymeric chains and subsequently decreasing porosity. DL wafers showed higher porosity between 90.50 ± 0.33% and 95.70 ± 0.98% than the BLK wafers (80.28 ± 1.45%). This could be due to the loading of drugs into the wafer matrix causing increased polymeric chain flexibility and hence, enhanced porosity compared to BLK wafers. The commercial dressing Actiformcool® did not show any porosity because of its hydrogel nature. Due to nonporous and high content of water (about 96%), hydrogel dressings cannot absorb enough exudates thus creating maceration in highly exudative wounds (Mavrogenis et al., 2018).

Table 2. Results for the porosity, EWC, Aw, WVTR and moisture content, of different formulations and the commercial dressing (n = 3 ± SD).

Formulation	Porosity (%)	EWC (%)	Aw (%)	WVTR (g/m^{2}day^{-1})	Moisture content (%)
CA-BLK F	38.34 ± 3.80	73.80 ± 0.55	281.85 ± 7.85	2919.32 ± 223.77	7.74 ± 0.51
CA-CIP:FLU (1:10) F	44.43 ± 3.85	74.57 ± 1.45	294.11 ± 18.21	1675.44 ± 104.93	11.86 ± 0.13
CA-CIP:FLU (1:20) F	42.34 ± 1.92	74.93 ± 0.79	299.28 ± 12.35	1647.18 ± 222.72	11.38 ± 0.08
CA-BLK W	80.28 ± 1.45	97.11 ± 0.14	3373.54 ± 169.85	2577.42 ± 261.98	13.28 ± 0.86
CA-CIP:FLU (1:10) W	90.50 ± 0.33	95.20 ± 0.39	1994.77 ± 160.19	1912.68 ± 36.96	14.01 ± 1.15
CA-CIP:FLU (1:20) W	93.09 ± 0.67	95.53 ± 0.29	2147.59 ± 141.45	1959.84 ± 34.99	13.74 ± 0.85
CA-CIP:FLU (1:30) W	95.70 ± 0.98	95.96 ± 0.11	2377.52 ± 70.77	2003.23 ± 56.21	14.11 ± 0.09
Actiformcool®	0.00	88.51 ± 0.83	774.82 ± 61.09	972.97 ± 172.30	-

3.3 Fluid handling properties

3.3.1 Swelling studies

In matrix-based systems, the drug is entrapped within the polymeric matrix where water penetration leads to hydration and swelling. The swelling effect helps in formation of rubbery region followed by disentanglement of polymer chains resulting in drug mobility at the diffusion layer rich in water leading to subsequent drug release from the matrix (Achenie & Pavurala, 2017). The swelling capacity (index) of the dressings is closely related to pore shape, size distribution and overall porosity, crystallinity, residual moisture content and surface pH (Negoro et al., 2016; Pawar et al., 2014; Vishal & Shivakumar, 2012). As shown in Fig. 6, the wafers exhibited high degree of swelling indicating strong SWF handling capacity and this is attributed to its porous matrix (confirmed by SEM).

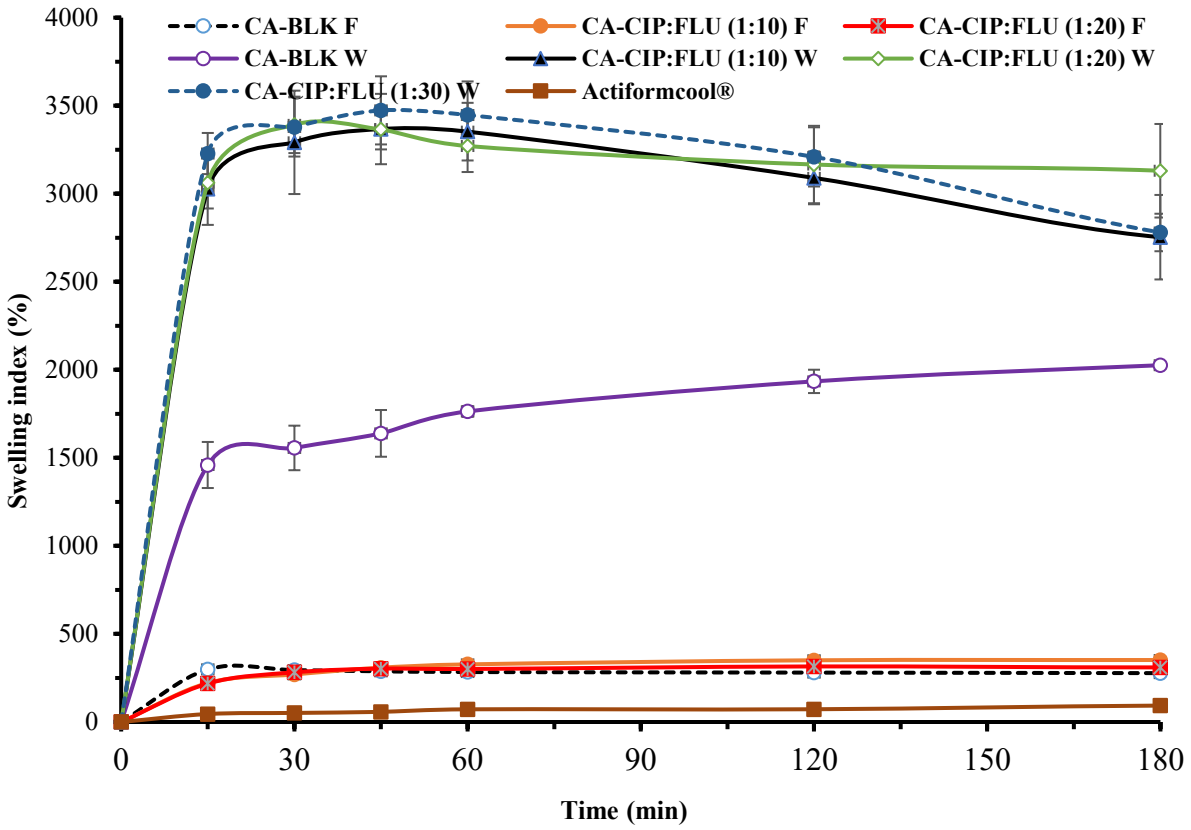

Fig. 6. Swelling index of BLK and DL films and wafers and the commercial hydrogel (Actiformcool®)

It was also evident that the DL wafers demonstrated significantly ($p < 0.05$) higher swelling than the BLK wafers which was due to hydrophilic nature of the drugs that boosted hydrogen bonding and hence enhanced hydration, resulting in higher percentage swelling. This may be related to the viscosity of the resulting gels (Fig. S1 – supplementary data), however, this requires further investigation. In addition, higher porosity of DL wafers (Table 2) enhanced the rate of water ingress. However, addition of drugs into the film matrix did not affect swelling properties in a significant way.

A rapid initial swelling rate was observed for all the formulated dressings during the first 15 min and after that the swelling rate attained equilibrium state after 30 min for films (BLK: 294.60 ± 8.30% and DL: about 276. 95%) and 60 min for wafers (BLK: 1763.78 ± 30.76% and DL: about 3356.93%). Subsequently, the swollen wafers slowly began to lose their structural consistency probably due to dissolution or erosion. Actiformcool® showed the lowest swelling capacity (about 45.28 – 93.16% over 180 min) amongst all formulated dressings because its high moisture content allowed for minimal water ingress into the swollen hydrogel matrix.

3.3.2 Water absorption (Aw) and equilibrium water content (EWC)

Aw and EWC represent the maximum water uptake and water holding capacity of the dressings respectively after 24 h. DL films showed Aw values between 294.11 ± 18.21% and 299.28 ± 12.35%, which was slightly more than the BLK films (281.85 ± 7.85). The higher absorption of DL films was attributed to the slightly higher porosity than BLK film (Table 2). Moreover, the addition of drugs increased hydrophilicity of the films resulting in higher water absorption. On the other hand, DL wafers showed significantly ($p < 0.05$) lower Aw (1994.77 - 2377.52 %) than BLK wafer (3373.54 ± 169.85). This could be due to loss of structural integrity of DL wafers after 24 h. Therefore, the frequency of wafer dressing change should ideally be performed daily to avoid excessive collection of exudates. There were no significant ($p > 0.05$) differences in EWC between BLK and DL films as well as BLK and DL wafers. This means that incorporation of drugs into the dressings had no impact on the fluid holding capacity. The commercial product Actiformcool® exhibited Aw of 774.82 ± 61.09% and EWC around 88.51 ± 0.83% which is low due to its high moisture content and being non-porous in nature.

3.3.3 Water vapour transmission rate (WVTR)

WVTR is an important characteristic for a dressing to ensure moist wound healing. Low WVTR of dressings may lead to maceration of healthy skin due to poor drainage of the absorbed wound fluid. On the other hand, high values of WVTR may cause drying out of the wound bed due to excess loss of fluid from the matrix of the swollen dressings. Therefore, to confirm the capability of moist wound healing, the formulated dressings and the commercial Actiformcool® were characterized in terms of WVTR (Lee et al., 2016). The WVTR (Table 2) of DL films ranged between 1647.18 ± 222.72 and 1675.44 ± 104.93 g/m^2day^{-1}, which indicating poor ability to take out fluid from the wound bed. The WVTR of DL wafers ranged from 1912.68 ± 36.96 to 2003.23 ± 56.21 g/m^2day^{-1}, indicating better vapour permeability than DL films due to its known porous nature which enabled capillary water transfer through the void space into the atmosphere. Therefore, the wafers will prevent the build-up of high volumes of exudate. WVTR of 2000-2500 g/m^2day^{-1} is a recommended rate to provide an adequate moisture level for wound healing without dehydration (Akiyode & Boateng, 2018). Therefore, it can be concluded that the combined (CIP/FLU) DL wafers would have the ability to maintain a moist wound environment. The commercial product Actiformcool® showed the lowest value WVTR (972.97 ±

172.30 g/m^{2}day^{-1}) due to its hydrophilic and dense non-porous nature resulting in low water escape. Therefore, hydrogel dressings have limitations when used in highly exuding wounds and are better suited for dry or low exuding wounds (Mavrogenis et al., 2018).

3.3.4 Evaporative water loss (EWL)

Once dressings get saturated with wound fluid, these need to be dehydrated to prevent maceration. The formulated film dressings demonstrated quick dehydration (52-72%) within 1 h (Fig. 6). After 1 h the films gradually dehydrated up to 2 h and retained 18% of water. The wafers showed EWL of 18-30% for the first hour and then gradual water loss was up to 6 h (Fig. 7) and then equilibrated at 8 h with 13-16% of water retention. This indicates that large volumes of exudate will be evaporated from the swollen wafers and at the same time retain some moisture which will help to prevent excess dehydration and subsequently will provide a moist wound environment. The study was extended to 24 h and it showed that the films retained 15-17% of moisture whereas the wafers retained 9-10% of moisture. The high water retention by films could be due to the plasticizing effect of GLY which is a known humectant. Actiformcool® exhibited very low water loss of about 20% after 8 h, which was lower than all the other formulated dressings. The high water retention ability of Actiformcool® was due to its three-dimensional structure, which possess hydrophilic properties resulting in higher affinity to retain water.

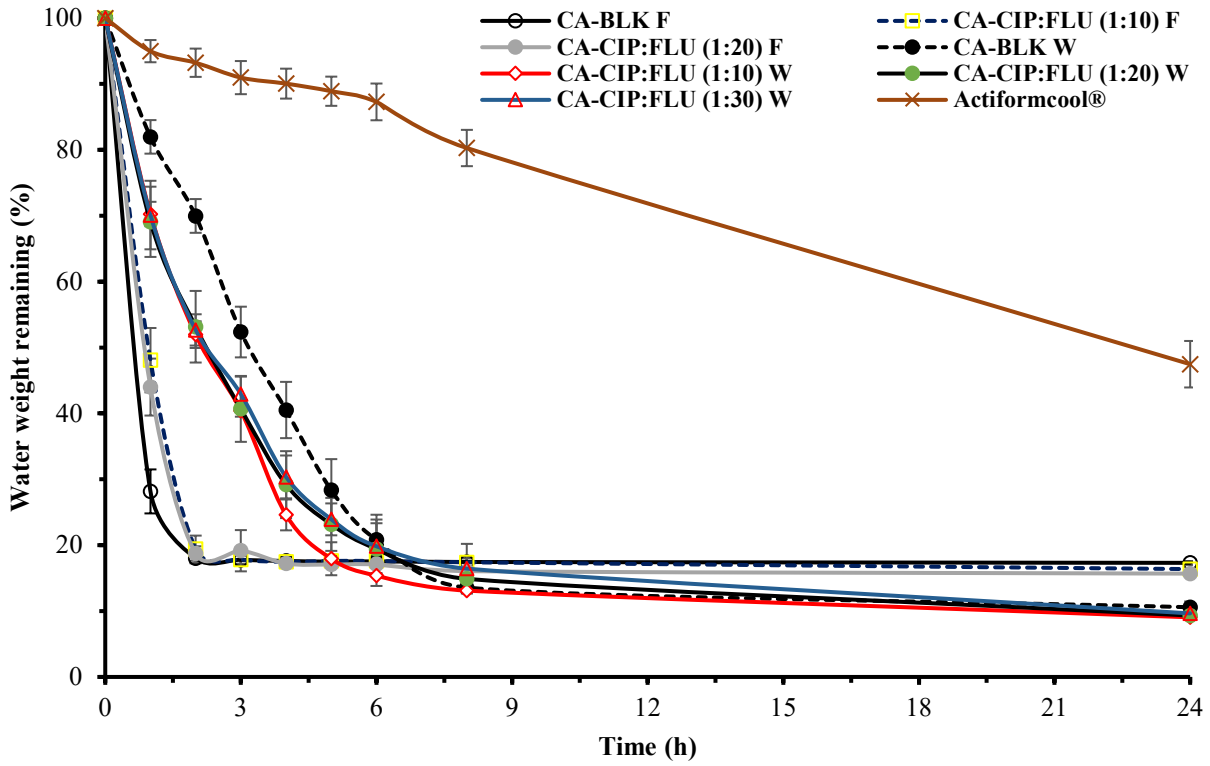

Fig. 7. EWL from formulated films, wafers and Actiformcool®

3.3.5 Moisture content

The residual moisture content of the formulated dressings is an important factor in terms of product stability and initial hydration of the wounds. From Table 2, it can be observed that the incorporation of drugs into the films and wafers influenced moisture content. The DL films showed significantly ($p < 0.05$) higher moisture content (11.38 ± 0.08 – 11.86 ± 0.13 %) than the BLK films (7.74 ± 0.51%). The higher moisture content in DL films was attributed to enhanced hydrophilicity which supported the higher bound water. In the case of wafers, the moisture content was slightly increased after loading of drugs and this could also be attributed to increase in hydrophilicity of the polymeric matrix after drug loading resulting in higher bound water. The hydrophilic groups present in CIP and FLU such as hydroxyls, carboxyls, amines and carbonyls (confirmed by FTIR) increase the hydrogen bonding between the drugs and CA molecules thus enhancing the surface wettability of the dressings. It was noted that the wafers exhibited higher residual moisture content than films overall. This was because in the final cycle of lyophilization, the wafers were dried at 20 °C whereas, in the solvent casting technique the films were dried at a higher temperature of 30 °C resulting higher residual moisture in wafers than the films.

3.4 In-vitro drug dissolution and release profiles

Fig. 8 shows the release profiles of (A) CIP and (B) FLU from the combined DL films and wafers. It can be observed that the release of CIP from the films was more controlled than FLU with maximum FLU release occurring soon after complete hydration (Fig. 8A). It was noted that, only 44.7 ±2.6% - 67.8 ±4.4% CIP was released from the CA-CIP:FLU (1:10) film over 360 min due to physical interactions with the polymer chains. The CIP release was higher (48.6 ± 3.5% - 90.5 ±1.6% over 360 min) in the CA-CIP:FLU (1:20) film than CA-CIP:FLU (1:10), suggesting that higher FLU loading resulted in higher CIP release. A similar pattern of CIP release was also observed in wafers containing CIP and FLU at the ratios of 1:10, 1:20 and 1:30 showing overall cumulative CIP release of 81.7 ± 2.3%, 88.1 ± 3.5% and 95.4 ± 2.7% respectively (Fig. 8A). This could be attributed to the higher amount of FLU reducing the physical interaction of CIP with the polymer molecules, followed by increasing entanglement of the polymer chains, resulting in higher CIP release. This interesting fact could also depend on porosity of the polymeric matrix as well as the solubility, ionic strength, and osmotic properties of the drugs (Sanopoulou & Papadokostaki, 2017).

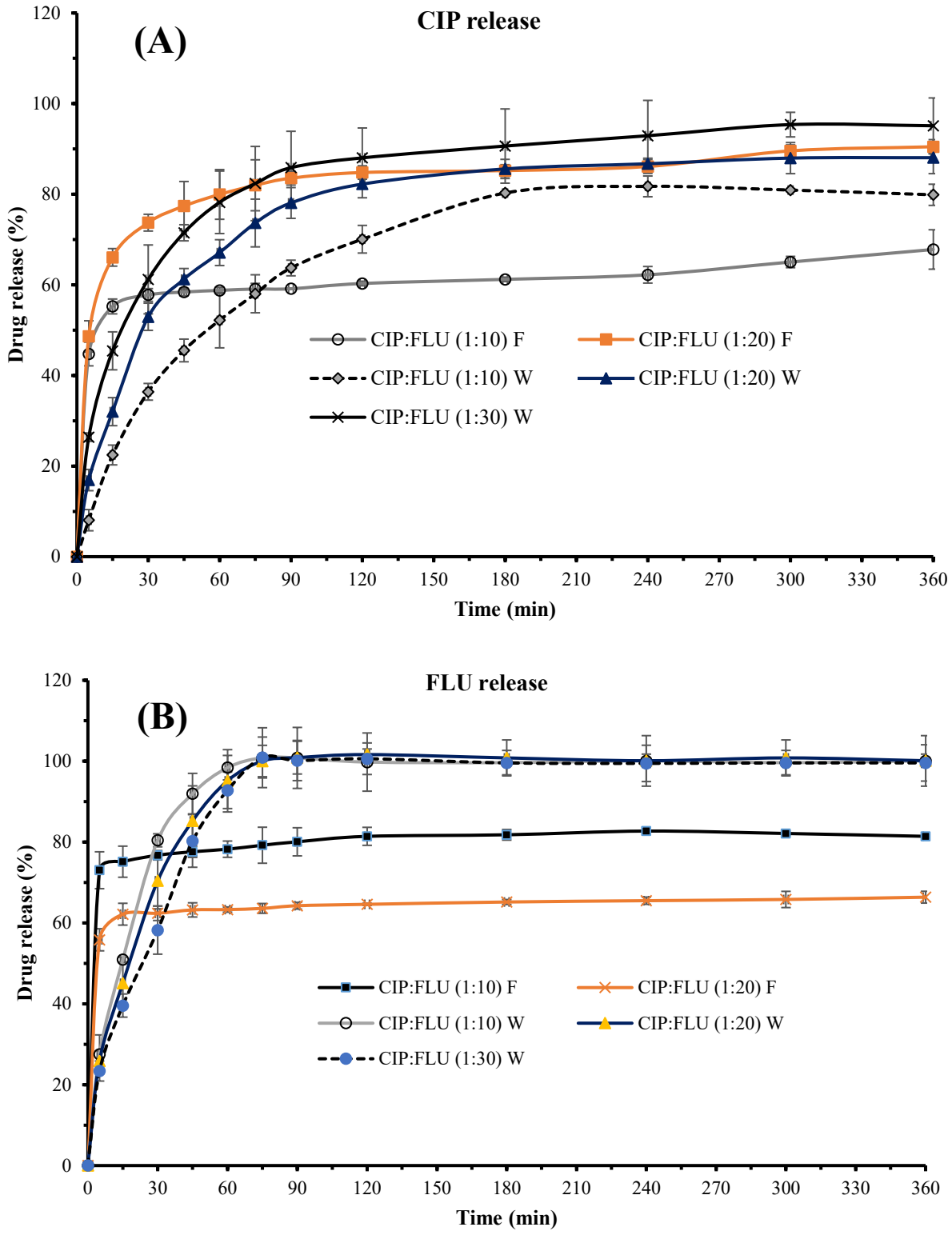

Fig. 8. *In vitro* drug release profiles of (A) CIP and (B) FLU from films and wafers containing both drugs in different ratios, showing mean percentage cumulative release (mean ± SD, $n = 3$) against time in the presence of SWF at pH 7.5

As shown in Table 2, higher amounts of FLU in combined DL wafers resulted in greater porosity, improved swelling and could be factors in the higher CIP release. In addition, the pore size of

swollen matrix might exceed the size of CIP molecules in the presence of higher amount of FLU. Furthermore, pH dependent solubility of CIP occurring at higher pH led to better solubility (Roca et al., 2015), evidenced by high surface pH of the DL films and wafers (Table S1).

On the other hand, higher release of FLU was observed (Figure 8B) in CA-CIP:FLU (1:10) film (82.7 ± 0.5%) than the film containing CIP and FLU at the ratio of 1:20 (66.4 ± 1.5%). This could be because the lower amount of FLU easily leached out from the film matrix due to relatively higher solubility in SWF than the formulations containing higher amount of FLU. It can be observed that FLU was released faster than CIP from the wafer matrix which could be due to difference in ionic properties of the drugs. FLU might have high affinity to the ions present in SWF creating a higher gradient for diffusion of FLU molecules more quickly from the swollen matrix. Moreover, it was previously reported that drugs having lower molecular weight diffused faster from matrices than drugs of higher molecular weight (Feng et al., 2015). This could have occurred in this study, as FLU of lower molecular weight (306.28 g/mol) diffused faster than CIP of higher molecular weight (331.35 g/mol). Furthermore, it is reported that FLU has higher solubility in PBS (pH 7.4) than water (pH 7.0) (Sakharam et al., 2012) while CIP has much lower solubility at pH 7.4 in PBS (Roca et al., 2015). This resulted in rapid initial (25% within 5 min) and maximum (100%) release of FLU (within 75 min). However, it will be useful in the future to compare the dissolution profiles of the non-encapsulated drugs (and their physical mixture) with the data collected from loaded films and wafers.

3.5 Mixed infection study

Mixed infection studies of combined DL (CIP and FLU) dressings were assessed by turbidimetric and *Kirby Bauer* disk diffusion methods. The turbidimetric study is based on the interaction between DL dressings and the test microorganisms (*E. coli*, *S. aureus*, *P. aeruginosa* and *C. albicans*), followed by changes in turbidity of the mixed microbial suspensions. As shown in Fig. 9A, the absorbance values of the mixed culture of *E. coli* and *C. albicans* gradually increased from 3h to 24 h confirming microbial growth. After 24 h, no significant increase in absorbance of the mixed culture (*E. coli* and *C. albicans*) was detected. The absorbance values of the BLK dressings and Actiformcool® also increased with time indicating promotion of microbial growth.

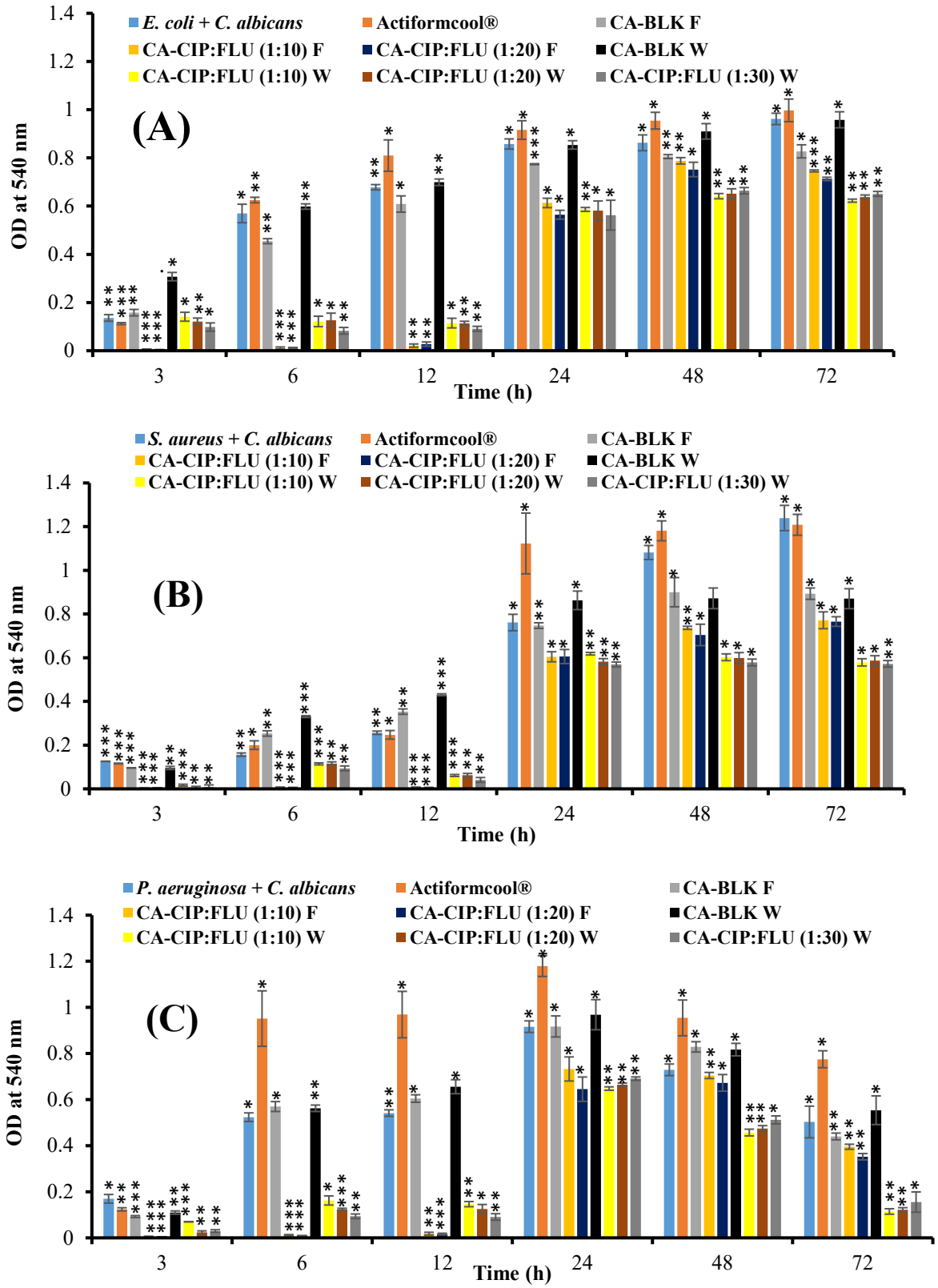

Fig. 9. Mean reading of increment at 540 nm wavelength optical density measurements of mixed bacterial and fungal strains treated with combined DL dressings and commercial product Actiformcool® ($n = 3 \pm$ SD). Asterisks (*) indicates the level of significance as *<0.05, ** <0.01 and ***<0.005. F: Film; W: Wafer

The absorbance values of the mixed infection (*E. coli* and *C. albicans*) treated with combined DL dressings were significantly lower ($p = 0.001$) than the positive control and BLK dressings up to 12 h. This confirms suppression of the mixed culture growth following release of both antimicrobials (CIP and FLU) from the dressings.

The absorbance value of the mixed culture comprising *S. aureus* and *C. albicans* gradually increased with time (Fig. 9B). This indicated that the *S. aureus* and *C. albicans* grew well together in the brain heart infusion broth. The gradual increase in cell densities could be due to interaction between *S. aureus* and *C. albicans* resulting in synergistic effect on their growth (Kean et al., 2017). This synergistic interaction hinders the healing of DFUs by enhancing microbial tolerance to the antimicrobial agents (Budzyńska et al., 2017). In this study, the growth of mixed culture of *S. aureus* and *C. albicans* was controlled up to 12 h when treated with combined DL dressings. This confirms that the synergistic action of the *S. aureus* and *C. albicans* was overcome by the combined DL dressings during this period. Moreover, the cell densities of mixed culture (*S. aureus* and *C. albicans*) treated with combined DL dressings were lower after 24 h compared to untreated mixed culture and BLK dressings indicating the effectiveness of the medicated dressings.

For the mixed culture of *P. aeruginosa* and *C. albicans,* the cell densities increased up to 24 h and after that the value decreased from 0.92 to 0.50 until 72 h (Fig. 9C) and the same observations were observed for the remaining samples. The reduction in cell densities might be due to antagonistic interaction of *P. aeruginosa* and *C. albicans* (Fourie et al., 2016). The interaction of *P. aeruginosa* and *C. albicans* is regulated by releasing of quorum sensing molecules from both organisms. However, *P. aeruginosa* could supress the growth of *C. albicans* by secreting chemical factors such as 5- methyl-phenazine-1-carboxylic acid which have anti-fungal properties. *C. albicans* can also inhibit the growth of *P. aeruginosa* by releasing quorum sensing molecules such as farnesol. Farnesol inhibits the production of *Pseudomonas* quinolone signal (PQS) that reduces pyochynin synthesis and swarming motility in *P. aeruginosa* (Dhamgaye et al., 2016).

Overall, the turbidity of the mixed cultures (*E. coli* and *C. albicans,* or *S. aureus* and *C. albicans,* or *P. aeruginosa* and *C. albicans*) treated with the dressings containing both CIP and FLU was significantly lower ($p < 0.05$) than the untreated mixed cultures. On the other hand, the turbidity of all mixed cultures treated with Actiformcool® were similar to the negative control and BLK dressings, which is attributed to the absence of antimicrobial agents in Actiformcool®. Overall, the results presented show that the combined DL dressings reduced growth of mixed bacterial and fungal infections and support its use against mixed infections.

The killing patterns of the dressings containing CIP and FLU are illustrated in the supplementary information (Fig. S5 A-F). It can be observed that the combined DL dressings killed 99.9% of the culture within 3 h (Fig. S5 A, C & E). This rapid killing of bacteria (*E. coli, S. aureus* and *P. aeruginosa*) was mediated by the maximum release of CIP from the dressings within a short time (Fig. 8A). The complete eradication of bacterial cells was observed within 24 h in case of the mixed

culture of *E. coli* and *C. albicans*, as well as *P. aeruginosa* and *C. albicans*. In the mixed culture of *S. aureus* and *C. albicans,* the complete eradication of bacteria was observed within 72 h and this delayed eradication of *S. aureus* might be due to the synergistic interaction between *S. aureus* and *C. albicans*.

Overall, the DL dressings appeared to be highly effective against the causative bacteria present in DFUs and the presence of *C. albicans* did not affect the antibacterial activity of the dressings significantly. In terms of killing *C. albicans* in the mixed cultures, combined DL dressings showed 10-fold reduction in cell numbers when compared to the control mixed cultures (untreated). Therefore, the combined DL dressings can eradicate 90% of fungal cells from the mixed infections. The highest survival was observed when the mixed cultures were treated with the commercial product Actiformcool®, confirming no antimicrobial activity. Moreover, the number of the viable cells of *C. albicans* in the presence of *P. aeruginosa* was 10^6 CFU/ml after 72 h (Fig. S5 F). Within the same incubation period, the viability of the fungal cells was higher in the mixed culture (*C. albicans* either with *E. coli* (10^8 CFU/ml) or *S. aureus* (10^9 CFU/ml)). It suggests that *P. aeruginosa* has antagonistic effects on the growth of *C. albicans* which was also supported by the turbidity assay results (Fig. 9C). The lowest number (10^5 CFU/ml) of viable fungal cells was observed when the mixed culture of *C. albicans* and *P. aeruginosa* was treated with combined DL dressings. In terms of antimicrobial activity both medicated dressings (films and wafers) showed similar responses against all the mixed cultures.

The ZOI assay mimics the clinical use of the antimicrobial products and predicts the capability of the dressings to kill or prevent microbial growth in a wound bed. Inoculated BHI agar plates represent an infected moist or exuding wound surface. To exhibit antimicrobial activity, the dressings need to absorb moisture from the colonized agar plates to trigger the drug (CIP and FLU) release from the swollen matrix. Thereafter, the drugs need to diffuse to the agar to exert its antimicrobial effect. Fig. S6 shows the inhibitory zone diameters of combined DL dressings placed on the mixed cultures of bacteria and fungi. The BLK dressings did not show any inhibitory effect on the mixed infections which was also confirmed by the turbidity (Fig. 9) and time-kill assays (Fig. S5). The dressings (wafers and films) containing CIP and FLU showed the strongest inhibitory effect (ZOI, 34.0 - 44.8 ± 0.2 nm) against the mixed culture of *P. aeruginosa* and *C. albicans* amongst all other mixed cultures. This high inhibitory effect was also enhanced by the antagonistic interaction between *P. aeruginosa* and *C. albicans*. The DL dressings had the lowest ZOI (26.5 - 36.5 ± 0.4 nm) against the mixed culture of *S. aureus* and *C. albicans* due to synergistic interaction of *S. aureus* and *C. albicans* in resisting drug antimicrobial action. The obtained results also showed that the wafers showed higher ZOI (36.7 - 44.8 ± 0.2 nm) than the films (26.5 - 35.6 ± 0.7 nm) against all mixed cultures (supplementary data – Fig. S6. This could be attributed to the higher drug release from the wafers than the films as shown in Fig. 8 above.

3.6 MTT assay

MTT assay revealed that PEK cells were viable after exposure to BLK and DL dressings (films and wafers) with over 90% and 80% respectively after 72 h of culture (Fig. 10**)**. It was observed that

the cell viability of PEK cells after exposure to BLK and combined DL dressings decreased with time, however, the different combined DL films and wafers did not show any significant differences (p > 0.05) in cell viability. The cell viability decreased with increasing amount of FLU in the combined DL dressings implying that the biocompatibility is dependent on the dose of FLU. However, none of the formulated combined DL dressings were considered cytotoxic according to ISO standard since all the combined DL dressings showed > 70% cell viability (Meneses et al., 2020).

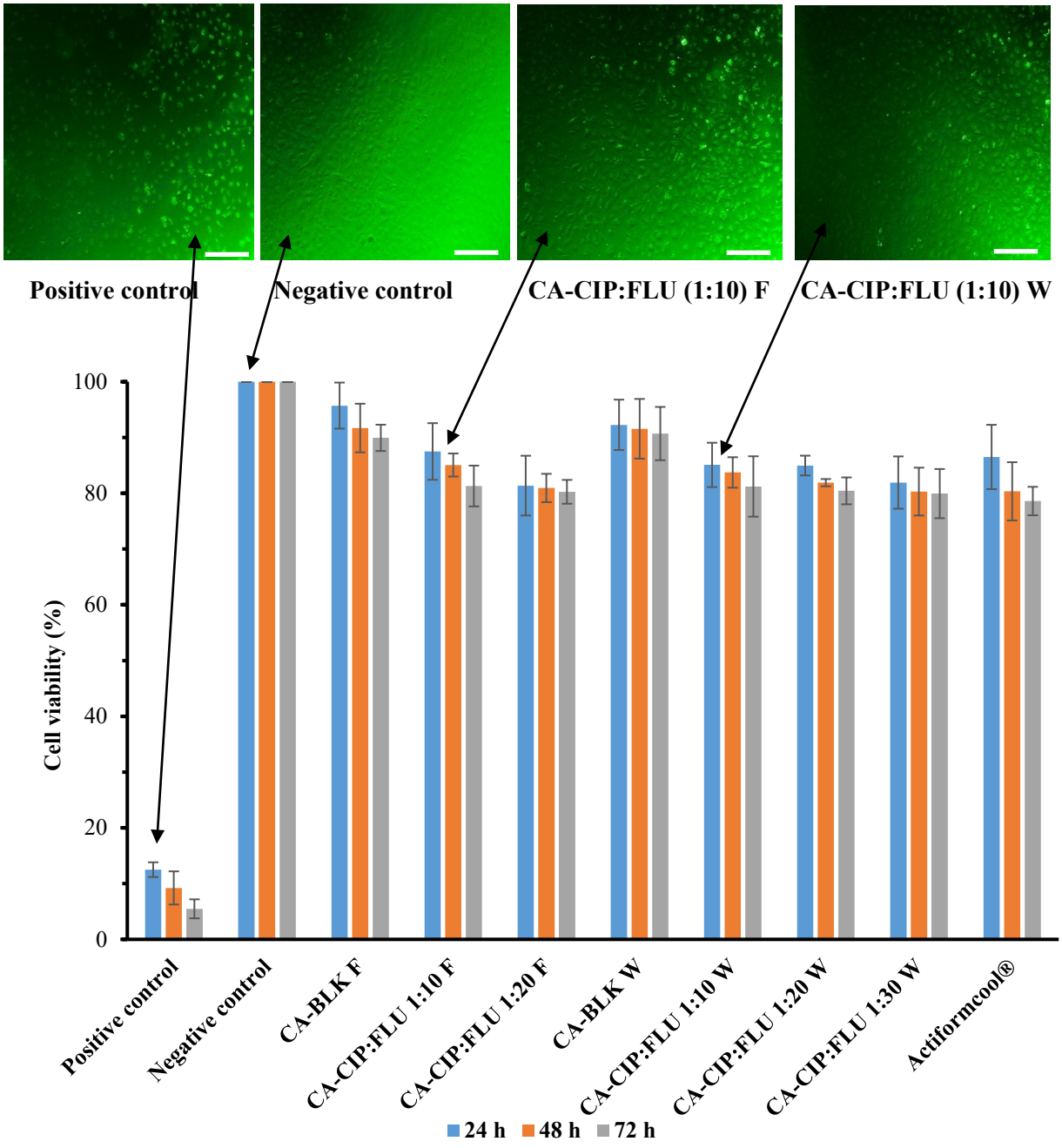

Fig. 10. Percentage of cell viability of human primary epidermal keratinocyte (PEK) cells after 24, 48 and 72 h of exposure to combined DL dressings and Actiformcool®. Triton-X-100 and untreated cells were used as positive and negative control respectively (n = 3 ± SD). Photomicrographs (4x) showing

the proliferation of human PEK cells after 24 h seeded at a density of 1 x 10^5 cells/ml with the combined DL dressings. F: Film; W: Wafer. Scale bar: 500 µm.

The cell viability of Actiformcool® was recorded at more than 85% after 24 h and about 80.4 ± 5.8% and 78.6 ± 2.6% after 48 and 72 h respectively, which is to be expected, since it is an approved commercial dressing using clinically. The untreated cells were considered as 100% viable and as expected, Triton-X-100 showed the highest toxicity with only 5% cell viability after 72 h of incubation. The cytotoxicity of Triton-X-100 is associated with the interaction between its monomer and the lipid bilayer present in the cells. The polar head group of Triton-X-100 reacts with lipophilic substances and phospholipids of cell membranes resulting in disruption of compactness and integrity of the lipid membrane, causing breakdown of cellular structure and ultimately leading to cell death (Koley & Bard, 2010).

Additionally, microscopic observation was carried out to assess the morphological changes of PEK cells after treating with the extracts of the DL dressings. The interaction between drugs and cells might cause cell death resulting in detachment of the cells from the surface of the culture plate. The polygonal shaped PEK cells grew confluent as a monolayer when treated with the dressings containing both CIP and FLU and the cells continued to grow uniformly over 72 h (Table S5). Though the confluence of PEK cells decreased after 72 h to some extent, there were no significant changes in morphology of PEK cells between combined DL films and wafers, which was also supported by the cell viability assay. Actiformcool® also demonstrated similar biocompatibility as the prepared dressings, therefore validated the experiment, while PEK cells treated with Triton-X-100 became shrunk, necrotic and detached from the culture plates.

3.7 Wound scratch (cell migration) assay

Migration of keratinocytes is important for wound healing because a wound cannot heal without reepithelialization. In chronic DFUs, keratinocytes experience hyperglycaemia and supraphysiological oxidative stress, which challenge their viability and migration (Xiao et al., 2016). Therefore, in this study the effect of the formulated dressings on human PEK cell migration was evaluated by an *in vitro* wound scratch assay.

As shown in Fig. 11, the PEK cells barely migrated into the wound gap (about 7.6 ± 2.0%) after 3 days of treating with Triton-X-100 (negative control). After 7 days, no cell migration was observed because all the surrounding cells within the wound gap had died (Table S6). In the case of untreated cells (positive control) PEK cell migration (wound closure) was about 81.5 ± 2.0% after 3 days and complete wound closure (100%) was observed after 7 days. The wound closure of the cells treated with BLK films and wafers was also completed by 7 days. It appears evident that CA polymer dressings were found to be safe for PEK cells which agrees with the cell viability study. As shown in Fig. 11 and Table S6, the medicated films and wafers exhibited wound closure about 65.0 ± 0.2% and 67.6 ± 6.7%

respectively after 7 days. The DL dressings showed reduced performance of wound closure compared to BLK possibly because of the interaction of drugs with cells which caused some cell death and subsequent detachment which impacted wound closure. The cell viability study also showed that the rate of cell death for BLK dressings was lower than that for DL dressings. Therefore, complete wound closure occurred for BLK films and wafers. This suggests that the dose of loaded drug needs to be calibrated appropriately to achieve therapeutic efficacy but also ensure safety to newly formed cells in the healing wound.

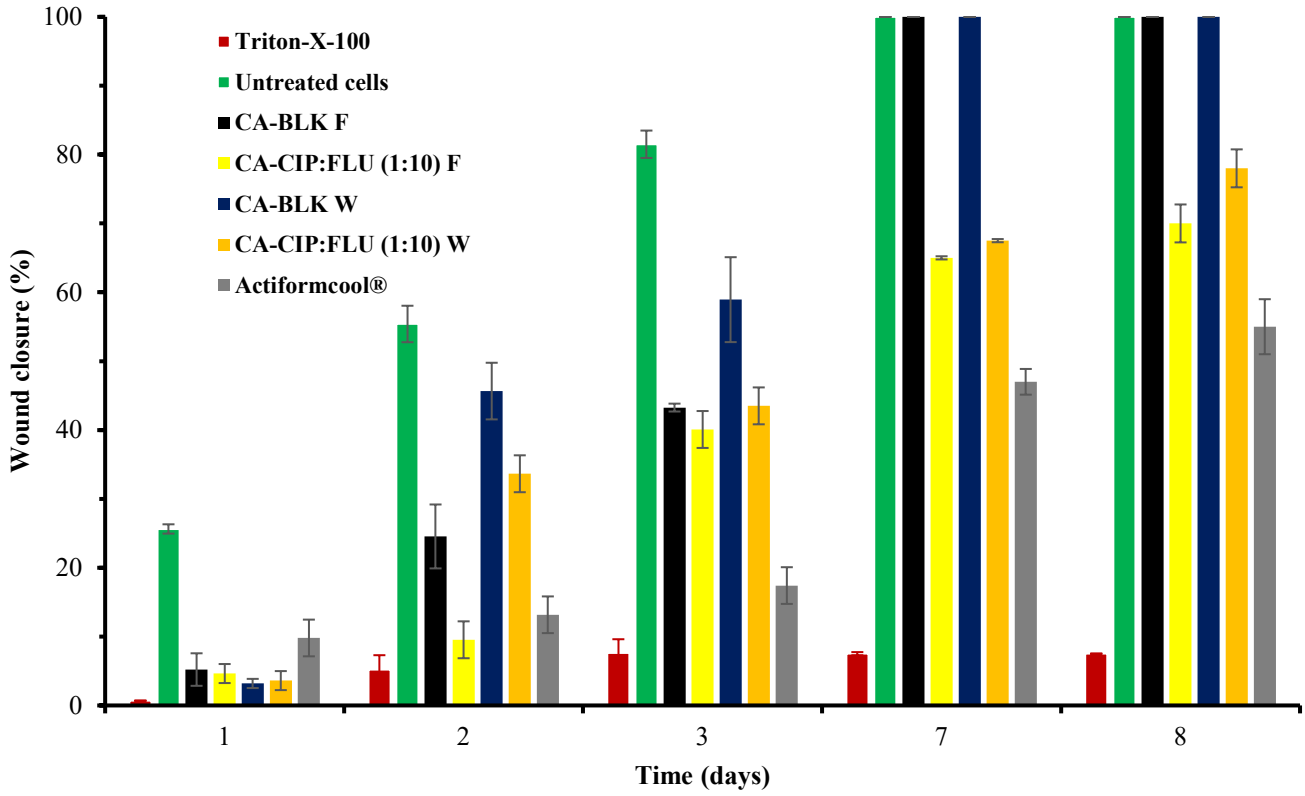

Fig. 11. *In vitro* wound scratch assay on human PEK cells treated with medicated films, wafers and Actiformcool® ($n = 3 \pm$ SD). F: Film; W: Wafer

Cells treated with the commercial product (Actiformcool®) showed slower rate of migration than the cells treated with formulated dressings. After 8 days of culture, representative wounds treated with Actiformcool® exhibited a wound closure of 55.0 ± 4.0% compared to the initial wound gap. Overall, the results obtained through wound scratch assay revealed that the alginate-based dressings had a positive effect on the *in vitro* wound closure rate and could play a potential role in wound healing applications. However, *in vivo* wound healing will need to be investigated to elucidate the effectiveness of the dressings.

4. Conclusions

In this study**,** alginate-based dressings (films and wafers) containing an antibacterial and an antifungal drug were successfully formulated and functionally characterised. The combined DL dressings exhibited desired physical and chemical properties required for effective wound healing. *In-vitro* drug release study demonstrated burst release of FLU and sustained release of CIP which will be expected to inhibit microbial growth rapidly as well as prevent reinfection due to controlled drug release. The combined DL dressings were found to be highly effective against the mixed infections and exhibited bactericidal activity (99.9% killing) within 3 h and 10-fold reduction (90% killing) of the fungal cells. The combined DL dressings showed > 70% cell viability which complies with the expected ISO standard. Moreover, wound closure greater than 65% was observed within 7 days after treatment with the medicated dressings. All the formulated dressings showed better functional wound dressing performance for potential wound healing in terms of fluid handling characteristics, antimicrobial activity, cell viability and migration than the commercial product Actiformcool®. In summary, this study demonstrated that the combination of antibacterial and antifungal drugs in a single dressing is feasible and could be suitable for the treatment of mixed infections in DFUs. However, other studies such as stability over time, contact angle goniometry studies to evaluate hydrophobicity/hydrophobicity, and hydration/dehydration studies using actual chronic ulcer exudate will be necessary in the future. In addition cell and bacterial/fungal studies using the controlled materials to compare with the final products as well as cell attachment and *in vivo* animal testing are required to elucidate the wound healing action of the prepared dressings.

Declarations of interest: None.

References

Achenie, L.E., Pavurala, N., 2017. Modelling of drug release from a polymer matrix system. 2 (3). https://doi.org/10.19080/NAPDD.2017.02.555589.

Aderibigbe, B.A., Buyana, B., 2018. Alginate in wound dressings. Pharmaceutics. 10 (2), 42. https://doi.org/10.3390/pharmaceutics10020042.

Afrashi, M., Nasari, M., Semnani, D., Dehghan, P., Maheronnaghsh, M., 2021. Comparison of the antifungal activity of fluconazole- and ketoconazole-loaded PCL/PVP nanofibrous mat. Bull. Mater. Sci. 44. https://doi.org/10.1007/s12034-021-02456-9.

Ahmad Raus, R., Wan Nawawi, W.M.F., Nasaruddin, R.R., 2021. Alginate and alginate composites for biomedical applications. Asian J. Pharm. 18:7 Sci. https://doi.org/10.1016/j.ajps.2020.10.001.

Ahmed, A., Boateng, J., 2020. Treatment of Mixed Infections in Wounds, in: Ther. Dressings Wound Heal. Appl. 91-113. https://doi.org/10.1002/9781119433316.ch5.

Ahmed, A., Boateng, J., 2018. Calcium alginate-based antimicrobial film dressings for potential healing of infected foot ulcers. Ther. Deliv. 9, 185–204. https://doi.org/10.4155/tde-2017-0104.

Ahmed, A., Getti, G., Boateng, J., 2018. Ciprofloxacin-loaded calcium alginate wafers prepared by freeze-drying technique for potential healing of chronic diabetic foot ulcers. Drug Deliv. Transl. Res. 8, 1751–1768. https://doi.org/10.1007/s13346-017-0445-9.

Akiyode, O., Boateng, J., 2018. Composite biopolymer-basedwafer dressings loaded with microbial biosurfactants for potential application in chronic wounds. Polymers (Basel). 10. https://doi.org/10.3390/polym10080918.

Amin, Z.M., Koh, S.P., Tan, C.P., Yeap, S.K., Hamid, N.S.A., Long, K., 2017. Evaluation of in vitro wound healing efficacy of breadfruit derived starch hydrolysate. Int. Food Res. J. 24, 1771-1781.

Anh, H.T.P., Huang, C.M., Huang, C.J., 2019. Intelligent Metal-Phenolic Metallogels as Dressings for Infected Wounds. Sci. Rep. 9. https://doi.org/10.1038/s41598-019-47978-9.

Boateng, J.S., Popescu, A.M., 2016. Composite bi-layered erodible films for potential ocular drug delivery. Colloids Surfaces B Biointerfaces. 145, 353-361. https://doi.org/10.1016/j.colsurfb.2016.05.014.

Budzyńska, A., Różalska, S., Sadowska, B., Różalska, B., 2017. Candida albicans/Staphylococcus aureus Dual-Species Biofilm as a Target for the Combination of Essential Oils and Fluconazole or Mupirocin. Mycopathologia.182, 989-995. https://doi.org/10.1007/s11046-017-0192-y.

Catanzano, O., Docking, R., Schofield, P., Boateng, J.S., 2017. Advanced multi-targeted composite biomaterial dressing for pain and infection control in chronic leg ulcers. Carbohydr. Polym. 172, 40-48. https://doi.org/10.1016/j.carbpol.2017.05.040.

Centkowska, K., Ławrecka, E., Sznitowska, M., 2020. Technology of orodispersible polymer films with micronized loratadine—influence of different drug loadings on film properties. Pharmaceutics 12. https://doi.org/10.3390/pharmaceutics12030250.

Chadwick, P., 2013. Fungal infection of the diabetic foot : The often ignored complication. Diabet. foot J. 16, 102–107.

Chellan, G., Shivaprakash, S., Ramaiyar, S. K., Varma, A. K., Varma, N., Sukumaran, M. T., Vasukutty, J. R., et al. (2010). Spectrum and prevalence of fungi infecting deep tissues of lower-limb wounds in patients with type 2 diabetes. Journal of Clinical Microbiology, 48(6), 2097-2102.

Cherng, J.-H., 2020. Calcium Alginate Polysaccharide Dressing as an Accelerated Treatment for Burn Wound Healing, in: Wound Healing. https://doi.org/10.5772/intechopen.80875.

Dhamgaye, S., Qu, Y., Peleg, A.Y., 2016. Polymicrobial infections involving clinically relevant Gram-negative bacteria and fungi. Cell. Microbiol. 18, 1716 - 1722. https://doi.org/10.1111/cmi.12674.

Dumville, J.C., Deshpande, S., O'Meara, S., Speak, K., 2013. Foam dressings for healing diabetic foot ulcers. Cochrane Database Syst. Rev. Cd009111. https://doi.org/10.1002/14651858.CD009111.pub3.

Fan, Y., Lüchow, M., Zhang, Y., Lin, J., Fortuin, L., Mohanty, S., Brauner, A., Malkoch, M., 2021. Nanogel Encapsulated Hydrogels As Advanced Wound Dressings for the Controlled Delivery of Antibiotics. Adv. Funct. Mater. 31. https://doi.org/10.1002/adfm.202006453.

Fang, Q., Yao, Z., Feng, L., Liu, T., Wei, S., Xu, P., Guo, R., Cheng, B., Wang, X., 2020. Antibiotic-loaded chitosan-gelatin scaffolds for infected seawater immersion wound healing. Int. J. Biol. Macromol. 159, 1140 - 1155. https://doi.org/10.1016/j.ijbiomac.2020.05.126.

Feng, S., Nie, L., Zou, P., Suo, J., 2015. Effects of drug and polymer molecular weight on drug release from PLGA-mPEG microspheres. J. Appl. Polym. Sci. 131. https://doi.org/10.1002/app.41431.

Fourie, R., Ells, R., Swart, C.W., Sebolai, O.M., Albertyn, J., Pohl, C.H., 2016. Candida albicans and Pseudomonas aeruginosa interaction, with focus on the role of eicosanoids. Front. Physiol. 7. https://doi.org/10.3389/fphys.2016.00064.

Gao, C., Pollet, E., Avérous, L., 2017. Properties of glycerol-plasticized alginate films obtained by thermo-mechanical mixing. Food Hydrocoll. 63, 414–420. https://doi.org/10.1016/j.foodhyd.2016.09.023

Hashemikia, S., Farhangpazhouh, F., Parsa, M., Hasan, M., Hassanzadeh, A., Hamidi, M., 2021. Fabrication of ciprofloxacin-loaded chitosan/polyethylene oxide/silica nanofibers for wound dressing application: In vitro and in vivo evaluations. Int. J. Pharm. 597. https://doi.org/10.1016/j.ijpharm.2021.120313.

Hsu, S.T., Yao, Y.L., 2014. Effect of film formation method and annealing on morphology and crystal structure of poly (L-Lactic Acid) films. J. Manuf. Sci. Eng. Trans. ASME 136. https://doi.org/10.1115/1.4025909.

Hussain, Z., Thu, H.E., Shuid, A.N., Katas, H., Hussain, F., 2017. Recent Advances in Polymer-based Wound Dressings for the Treatment of Diabetic Foot Ulcer: An Overview of State-of-the-art. Curr. Drug Targets 19, 527 - 550. https://doi.org/10.2174/1389450118666170704132523.

Kalan, L., Grice, E.A., 2018. Fungi in the wound microbiome. Adv. Wound Care. 7, 247-255. https://doi.org/10.1089/wound.2017.0756.

Kean, R., Rajendran, R., Haggarty, J., Townsend, E.M., Short, B., Burgess, K.E., Lang, S., Millington, O., Mackay, W.G., Williams, C., Ramage, G., 2017. Candida albicans mycofilms support Staphylococcus aureus colonization and enhances miconazole resistance in dual-species interactions. Front. Microbiol. 8. https://doi.org/10.3389/fmicb.2017.00258.

Karthikeyan, K., Sowjanya, R.S., Yugandhar, A.D. V., Gopinath, S., Korrapati, P.S., 2015. Design and development of a topical dosage form for the convenient delivery of electrospun drug loaded nanofibers. RSC Adv. 5, 52420–52426. https://doi.org/10.1039/C5RA04438C.

Koley, D., Bard, A.J., 2010. Triton X-100 concentration effects on membrane permeability of a single HeLa cell by scanning electrochemical microscopy (SECM). Proc. Natl. Acad. Sci. U. S. A. 107 (39), 16783-167787. https://doi.org/10.1073/pnas.1011614107.

Mavrogenis, A.F., Megaloikonomos, P.D., Antoniadou, T., Igoumenou, V.G., Panagopoulos, G.N., Dimopoulos, L., Moulakakis, K.G., Sfyroeras, G.S., Lazaris, A., 2018. Current concepts for the evaluation and management of diabetic foot ulcers. EFORT Open Rev. 3, 513 - 525. https://doi.org/10.1302/2058-5241.3.180010.

Meneses, J., Silva, J.C., Fernandes, S.R., Datta, A., Ferreira, F.C., Moura, C., Amado, S., Alves, N., Pascoal-Faria, P., 2020. A multimodal stimulation cell culture bioreactor for tissue engineering: A numerical modelling approach. Polymers (Basel). 12. https://doi.org/10.3390/POLYM12040940

Mohandas, A., Deepthi, S., Biswas, R., Jayakumar, R., 2018. Chitosan based metallic nanocomposite scaffolds as antimicrobial wound dressings. Bioact. Mater. 3(3), 267-277. https://doi.org/10.1016/j.bioactmat.2017.11.003.

Moore, K., 2006. The interaction of a 'second generation' hydrogel with the chronic wound environment. Poster Presentation, EWMA Conference, Prague. Available at http://lohmann-rauscher.co.uk/downloads/clinical-evidence/AFC014-Keith-Moore-The-interaction-of-a-2nd-generation-h.pdf. [Accessed 29 January, 2018].

Nair, N., Biswas, R., Götz, F., Biswas, L., 2014. Impact of Staphylococcus aureus on pathogenesis in polymicrobial infections. Infect. Immun. 82(6), 2162-2169. https://doi.org/10.1128/IAI.00059-14.

Negoro, T., Thodsaratpreeyakul, W., Takada, Y., Thumsorn, S., Inoya, H., Hamada, H., 2016. Role of Crystallinity on Moisture Absorption and Mechanical Performance of Recycled PET Compounds, in: Energy Procedia. 89, 323–327. https://doi.org/10.1016/j.egypro.2016.05.042.

Ng, S., 2020. Freeze-Dried Wafers for Wound Healing, in: Therapeutic Dressings and Wound Healing Applications. https://doi.org/10.1002/9781119433316.ch7.

Paladini, F., De Simone, S., Sannino, A., Pollini, M., 2014. Antibacterial and antifungal dressings obtained by photochemical deposition of silver nanoparticles. J. Appl. Polym. Sci. 131. https://doi.org/10.1002/app.40326.

Pawar, H. V., Boateng, J.S., Ayensu, I., Tetteh, J., 2014. Multifunctional medicated lyophilised wafer dressing for effective chronic wound healing. J. Pharm. Sci. 103 (6), 1720–1733. https://doi.org/10.1002/jps.23968

Pawar, H. V., Tetteh, J., Boateng, J.S., 2013. Preparation, optimisation and characterisation of novel wound healing film dressings loaded with streptomycin and diclofenac. Colloids Surfaces B Biointerfaces 102, 102–110. https://doi.org/10.1016/j.colsurfb.2012.08.014

Peters, B.M., Noverra, M.C., 2013. Candida albicans-staphylococcus aureus polymicrobial peritonitis modulates host innate immunity. Infect. Immun. 81(6), 2178–2189. https://doi.org/10.1128/IAI.00265-13.

Peterson, L. R., Lissack, L. M., Canter, K., Fasching, C. E., Clabots, C., & Gerding, D. N. (1989). Therapy of lower extremity infections with ciprofloxacin in patients with diabetes mellitus, peripheral vascular disease, or both. The American Journal of Medicine, 86(6), 801-808.

Phoudee, W., Wattanakaroon, W., 2015. Development of Protein-Based Hydrogel Wound Dressing Impregnated With Bioactive Compounds. Natural Science, 49(1), 92-102.

Ramirez-Acuña, J.M., Cardenas-Cadena, S.A., Marquez-Salas, P.A., Garza-Veloz, I., Perez-Favila, A., Cid-Baez, M.A., Flores-Morales, V., Martinez-Fierro, M.L., 2019. Diabetic foot ulcers: Current advances in antimicrobial therapies and emerging treatments. Antibiotics. 8 (4), 193. https://doi.org/10.3390/antibiotics8040193.

Rewak-Soroczynska, J., Sobierajska, P., Targonska, S., Piecuch, A., Grosman, L., Rachuna, J., Wasik, S., Arabski, M., Ogorek, R., Wiglusz, R.J., 2021. New approach to antifungal activity of fluconazole incorporated into the porous 6-anhydro-α-l-galacto-β-d-galactan structures modified with nanohydroxyapatite for chronic-wound treatments—in vitro evaluation. Int. J. Mol. Sci. 22. https://doi.org/10.3390/ijms22063112.

Rezvanian, M., Tan, C.K., Ng, S.F., 2016. Simvastatin-loaded lyophilized wafers as a potential dressing for chronic wounds. Drug Dev. Ind. Pharm. 42(12), 2055–2062. https://doi.org/10.1080/03639045.2016.1195400.

Roca Jalil, M.E., Baschini, M., Sapag, K., 2015. Influence of pH and antibiotic solubility on the removal of ciprofloxacin from aqueous media using montmorillonite. Appl. Clay Sci. 114, 69–76.https://doi.org/10.1016/j.clay.2015.05.010

Sakharam, S.S., Shete, A.S., Patil Manisha, V., Varne Bhushan, S., 2012. Different binary polymer mixture for solubility enhancement of poorly water soluble drug by solid dispersion technique. Int. J. PharmTech Res. 4(3), 1159–1166.

Sanniyasi, S., Balu, J., Narayanan, C.D., 2015. Fungal Infection: A Hidden Enemy in Diabetic Foot Ulcers. Ankle Surg 2 (2), 74–76. https://doi.org/10.5005/jp-journals-10040-1033.

Sanopoulou, M., Papadokostaki, K.G., 2017. Controlled drug release systems: Mechanisms and kinetics, in: Biomedical Membranes And (Bio)Artificial Organs. https://doi.org/10.1142/9789813223974_0001.

Sarheed, O., Ahmed, A., Shouqair, D., Boateng, J., 2016. Antimicrobial Dressings for Improving Wound Healing, in: Vlad Adrian Alexandrescu (Ed.), Wound Healing - New Insights into Ancient Challenges. InTech, pp. 377–402. https://doi.org/10.5772/63961.

Sarwar, M.S., Ghaffar, A., Huang, Q., 2021. Development and characterization of sodium alginate/poly(sodium 4-styrenesulfonate) composite films for release behavior of ciprofloxacin hydrogen chloride monohydrate. Polym. Polym. Compos. https://doi.org/10.1177/0967391121990278.

Satish, A., Korrapati, P.S., 2015. Fabrication of a triiodothyronine incorporated nanofibrous biomaterial: Its implications on wound healing. RSC Adv. 5, 83773–83780. https://doi.org/10.1039/c5ra14142g

Taskin, A.K., Yasar, M., Ozaydin, I., Kaya, B., Bat, O., Ankarali, S., Yildirim, U., Aydin, M., 2013. The hemostatic effect of calcium alginate in experimental splenic injury model. Ulus. Travma Acil Cerrahi Derg. 19 (3), 195–199. https://doi.org/10.5505/tjtes.2013.30676.

Thattaruparambil Raveendran, N., Mohandas, A., Ramachandran Menon, R., Somasekharan Menon, A., Biswas, R., Jayakumar, R., 2019. Ciprofloxacin-and Fluconazole-Containing Fibrin-Nanoparticle-Incorporated Chitosan Bandages for the Treatment of Polymicrobial Wound Infections. ACS Appl. Bio Mater. 2, 243 - 254. https://doi.org/10.1021/acsabm.8b00585.

Vishal Gupta, N., Shivakumar, H.G., 2012. Investigation of Swelling Behavior and Mechanical Properties of a pH-Sensitive Superporous Hydrogel Composite. Iran. J. Pharm. Res. 11(2), 481–493. https://doi.org/10.1021/la980982.

Xiao, Y., Reis, L.A., Feric, N., Knee, E.J., Gu, J., Cao, S., Laschinger, C., Londono, C., Antolovich, J., McGuigan, A.P., Radisic, M., 2016. Diabetic wound regeneration using peptide-modified hydrogels to target re-epithelialization. Proc. Natl. Acad. Sci. 113(40), 5792–5801https://doi.org/10.1073/pnas.1612277113.

Yonashiro Marcelino, M., Azevedo Borges, F., Martins Costa, A.F., De Lacorte Singulani, J., Ribeiro, N.V., Barcelos Costa-Orlandi, C., Garms, B.C., Soares Mendes-Giannini, M.J., Herculano, R.D., Fusco-Almeida, A.M., 2018. Antifungal activity of fluconazole-loaded natural rubber latex against Candida albicans. Future Microbiol. 13. https://doi.org/10.2217/fmb-2017-0154.

Zhang, P.J., Jing, L.Y., Tang, S.|D., Zhu, Y.B., 2017. Global epidemiology of diabetic foot ulceration: a systematic review and meta-analysis†, Ann. Med. 49 (2017) 106–116. https://doi.org/10.1080/07853890.2016.1231932.

Supplementary information

Medicated multi-targeted alginate-based dressings for potential treatment of mixed bacterial and fungal infections in diabetic foot ulcers.

Asif Ahmed, Giulia Getti, Joshua Boateng*

School of Science, Faculty of Engineering and Science, University of Greenwich, Medway, Central Ave. Chatham Maritime, Kent ME4 4TB, UK.

* Correspondence: Dr Joshua Boateng (J.S.Boateng@gre.ac.uk; joshboat40@gmail.com)

Declarations of interest: None

Methods

Rheological characterization of gels

The viscosity of blank, plasticized and drug loaded gels was measured on an Anton-Parr MCR302 instrument with parallel plate geometry (PP25). Gels were sheared using a logarithmic ramp at shear rates from 0.1 – 100 Pa) at a temperature of 35°C and shear rate plotted against the shear stress.

Surface pH

The surface pH was determined by dipping the dressings in 10 ml of water and allowed to hydrate for 2 h at 37 °C. After that, the pH was detected by touching the surface of the hydrated dressings with the electrode of a pH meter (Mettler Toledo, UK) (Okoye & Okolie, 2015).

Drug content uniformity and drug loading efficiency

The ideal dressing should have uniform distribution of drug throughout the matrix to achieve minimum inhibitory concentration (MIC). Drug content uniformity was investigated by cutting the films into circular strips (6 mm diameter) and the wafers were cut into portions from three different locations and accurately weighed (~ 1-1.5 mg). The cut portions of film and wafer were placed in 2 ml of HPLC grade purified water. For drug loading efficiency the whole film was dissolved in 50 ml and wafer in 10 ml of HPLC grade purified water, respectively. The dressings were hydrated at 37 ºC with continuous stirring overnight to ensure complete drug dissolution. The sample solutions were filtered through 0.2 µm filter and were analysed by HPLC. The drug loading efficiency was calculated using Eq S1:

$$\text{Drug loading efficiency (\%)} = \frac{\text{total actual drug content}}{\text{amount of theoretical drug loading}} \text{ x } 100 \qquad \text{(S1)}$$

Determining minimum inhibitory concentration (MIC) and minimum fungicidal concentration of fluconazole (FLU)

The MIC of CIP was determined as in previously reported study (Ahmed et al., 2018). The MIC of pure FLU against *C. albicans* was also determined by broth dilution method in Sabouraud dextrose broth (Maheronnaghsh et al., 2016). The antifungal agent FLU was dissolved in ethanol at a final concentration of 1 mg/ml. Eleven 2-fold serial dilutions were prepared in Sabouraud dextrose broth medium, with final drug concentrations ranging from 0.06 to 64 µg/ml of FLU. Each concentration was tested in triplicate for the inoculum of 10^5 CFU/ml *C. albicans*. One of the tubes containing only fungal suspension without drug was used as a growth control. The tubes were incubated in a shaking incubator at 30 ºC for 24 h. After the incubation period, the tubes were observed visually to see the visible inhibition of the growth to determine MIC of FLU. Afterwards, to determine MFC, 100 µl of the treated fungal suspension was transferred from all clear tubes onto SB agar plates. The plates were then incubated at 30 ºC for 24 h. After 24 h, CFUs were counted and the number of viable cells was calculated using Eq S2. The MFC was considered as the lowest drug concentration that killed 99 – 99.5% of fungal cells (Maheronnaghsh et al., 2016).

Number of cell (CFU/ml) = (colonies counted x dilution factor)/ volume plated (S2)

Results and Discussion

Rheological characterization of gels

All the gels showed shear thinning behaviour with viscosity decreasing with shear (Fig. S1). This suggests that they will form free flowing gels upon hydration, however, given that the level of stress on a wound surface is minimal, this might not be an issue, except in frequently used areas such as arms and legs.

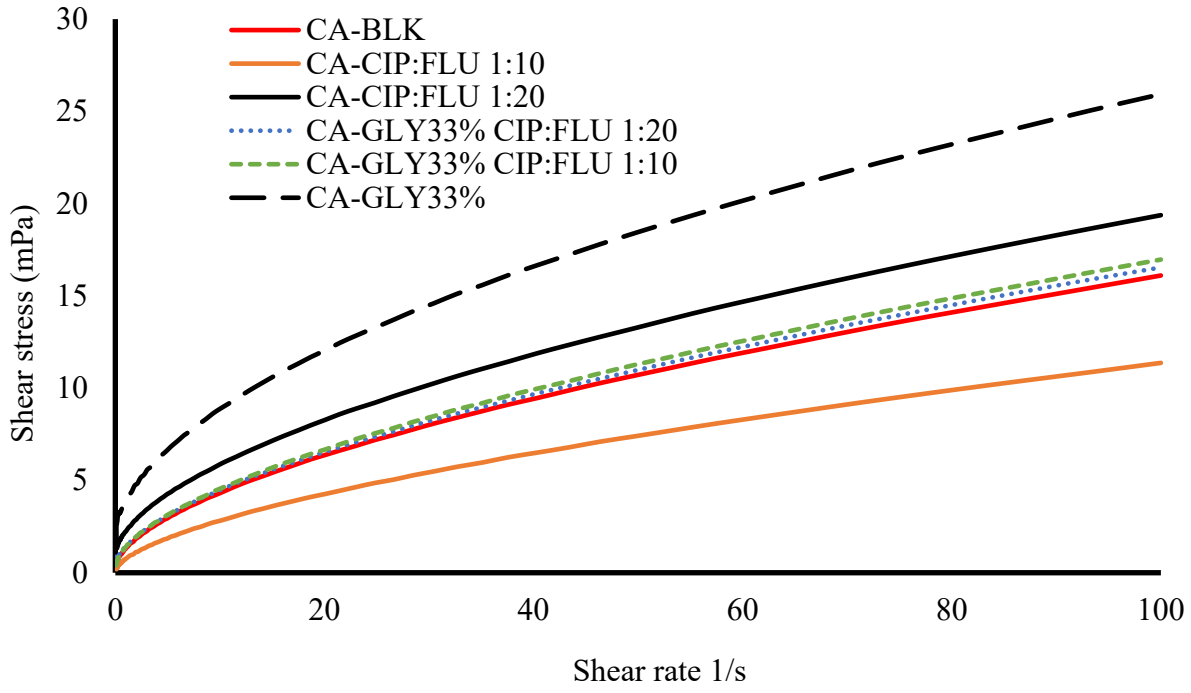

Fig. S1. Viscosity profiles of blank, plasticized and drug loaded gels, showing shear thinning behaviour.

There was no particular trend with different variables, however, generally, presence of GLY and high FLU content, increased the viscosity values at a given shear rate. Interestingly, the viscosity profiles for the different gels appear similar to the swelling profiles (Figure 5) of the corresponding wafers.

Surface pH

Surface pH of dressings is a contributing factor for effective wound healing with chronic DFUs having a pH range of 7.5 – 8.0 (McArdle et al., 2014). At elevated alkaline pH, the activity of proteolytic enzymes such as matrix –metalloproteases, increases, resulting in a prolonged inflammatory state, which subsequently enhances chronicity of the wounds (Schneider et al., 2007). Therefore, an effective wound healing approach is to reduce the pH level in the wound bed that will suppress the MMP enzyme activity. The DL films and wafers exhibited surface pH values 6.7- 7.0 and 7.1-7.4 (Table S1) respectively which can slightly decrease the elevated pH range (7.3 – 8.4) of DFUs. Studies revealed that the optimum cell proliferation and migration of keratinocytes and fibroblasts occurred at neutral pH around the body's internal pH of 7.4 and cell proliferation is affected at values above and below this pH (Topman et al., 2012). Therefore, the formulated DL dressings will be expected not to interfere with the proliferation and migration of fibroblasts and keratinocytes which are essential for wound healing. It was also reported that polymeric matrices exhibit high swelling at pH between 6.2 and 7.4 (Vishal Gupta and Shivakumar, 2012) which was in good agreement with this study. The CA-BLK films and wafers had a surface pH of 9.5 ± 0.2 and 9.2 ± 0.1 respectively whilst addition of drugs reduced the pH value due to presence of acidic functional groups in CIP and FLU. The surface pH of Actiformcool®

was found to be 5.9 ± 0.2 which can reduce the elevated protease activity and return the wound to a healing state.

Table S1. The surface pH of different formulations and the commercial dressing (n = 3 ± SD).

Formulation	Surface pH
CA-BLK F	9.53 ± 0.18
CA-CIP:FLU (1:10) F	6.71 ± 0.02
CA-CIP:FLU (1:20) F	7.01 ± 0.07
CA-BLK W	9.24 ± 0.09
CA-CIP:FLU (1:10) W	7.07 ± 0.20
CA-CIP:FLU (1:20) W	7.39 ± 0.18
CA-CIP:FLU (1:30) W	7.44 ± 0.09
Actiformcool®	5.91 ± 0.20

Drug content uniformity and drug loading efficiency

In order to verify the content of drugs in the dressings, drug loading efficiency was calculated with reference to theoretical content and illustrated in **Fig. S2**. The film containing CIP and FLU at the ratio of 1:10 showed CIP and FLU content about 64.0 ± 3.0% and 89.0 ± 1.0% respectively. It indicates that the low amount of FLU was well incorporated into the film sheet. However, films containing CIP and FLU at the ratio of 1:20 exhibited significantly higher ($p < 0.05$) CIP loading (91.0 ± 4.2%) than the film containing CIP and FLU in the ratio of 1:20. This could be explained by the fact that the addition of high amount of FLU (0.10%) with CIP resulted in increasing hydrogen bonding that enhanced the miscibility between the drugs within the film matrix. In the case of wafers, the amount of CIP and FLU was found to be similar in the wafers containing CIP and FLU at the ratio of 1:10 and 1: 20 whereas the recovery of FLU was low (70.5 ± 1.3%) in the wafer loaded with CIP and FLU at the ratio of 1:30. Furthermore, it can be observed (Fig. S2) that the wafers have the higher drug loading capacity than films as was previously documented by Boateng and co-workers (Ayensu *et al*., 2012a). The drug loading capacity depends on the porous network of lyophilized wafers (Ayensu *et al*., 2012b). The wafers can maintain the volume, size and shape of the original gel poured due to the freezing stage of free-drying, while films shrink due to evaporation during solvent casting. The lyophilization process yields porous wafers in which drug molecules can be entrapped whereas, oven drying process makes the films a continuous dense sheet resulting in less entrapment within the matrix and precipitation of excess drug on the surface of the films some of which can be lost through scraping and contact during handling (Boateng *et al*., 2012).

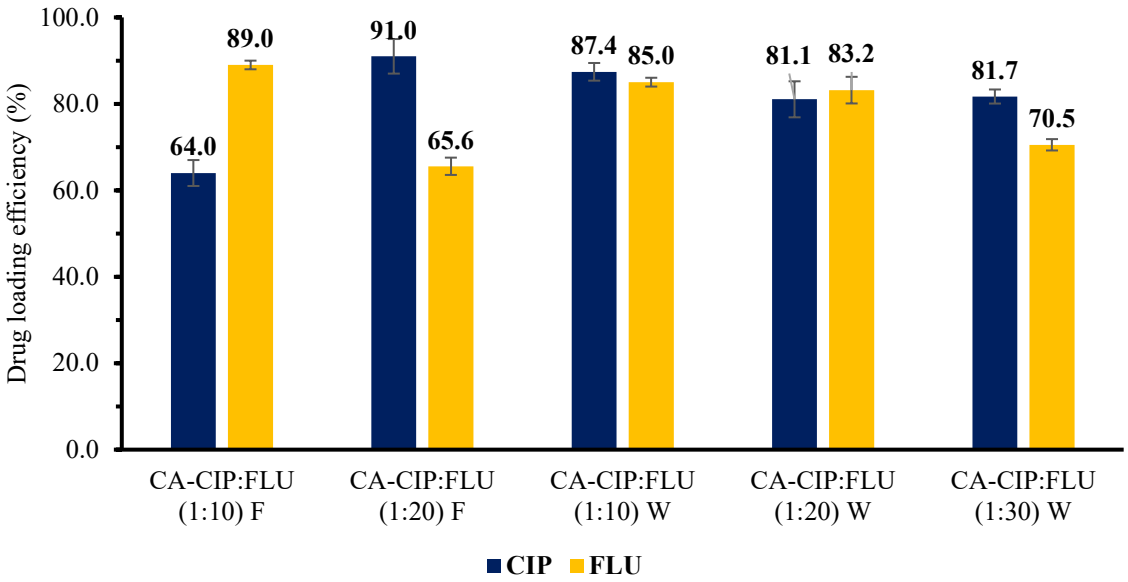

Fig. S2. Drug loading efficiency of formulated DL films and wafers ($n = 3 \pm$ SD).

In addition to drug loading efficiency, the drug content uniformity in the formulated dressings was analysed to investigate the distribution of drugs throughout the dressings. From the statistical evaluation of drug content uniformity of the combined DL dressings (Table S2), it was found that there were no significant differences ($p > 0.05$) in content of CIP and FLU on different parts of the dressings, which confirmed the biocompatibility between two drugs. Hence, it ensures the dosing accuracy.

Table S2. Observation of statistical differences in drug content uniformity of the dressings containing both CIP and FLU ($n = 3 \pm SD$).

Formulation	**Drug content (µg)**						***p* value**	
	P1		**P2**		**P3**			
	CIP	**FLU**	**CIP**	**FLU**	**CIP**	**FLU**	**CIP**	**FLU**
CA-CIP:FLU (1:10) F	4.7 ± 0.1	63.6 ± 0.3	4.8 ± 0.0	61.5 ± 0.2	4.6 ± 0.0	63.6 ± 0.0	> 0.05	> 0.05
CA-CIP:FLU (1:20) F	6.7 ± 0.0	92.9 ± 0.7	6.6 ± 0.0	92.1 ± 0.1	6.7 ± 0.0	94.2 ± 0.5	> 0.05	> 0.05
CA-CIP:FLU (1:10) W	3.1 ± 0.1	40.8 ± 0.1	3.1 ± 0.0	35.2 ± 0.1	3.0 ± 0.0	38.6 ± 0.1	> 0.05	> 0.05
CA-CIP:FLU (1:20) W	2.6 ± 0.0	77.9 ± 0.1	2.6 ± 0.0	75.3 ± 0.1	2.5 ± 0.0	78.2 ± 0.2	> 0.05	> 0.05
CA-CIP:FLU (1:30) W	2.1 ± 0.0	107.9 ± 0.1	2.5 ± 0.0	109 ± 0.2	2.3 ± 0.0	106.4 ± 0.1	> 0.05	> 0.05

Minimum inhibitory concentration (MIC) and minimum fungicidal concentration (MFC) of fluconazole (FLU)

The MIC value of FLU was found as 2 µg/ml for *C. albicans* (Fig. S3). The MFC range (2-512 µg/ml) of FLU was further evaluated to determine the MFC value. It was found that FLU killed 99.9% cells (1 x 10^4 CFU/ml) at a concentration of 128 µg/ml while comparing with the control (drug free culture) (2 x 10^8 CFU/ml) (Fig. S4). The comparative analysis of MIC and MFC indicated that MFC of FLU was six times greater than MIC for *C. albicans*.

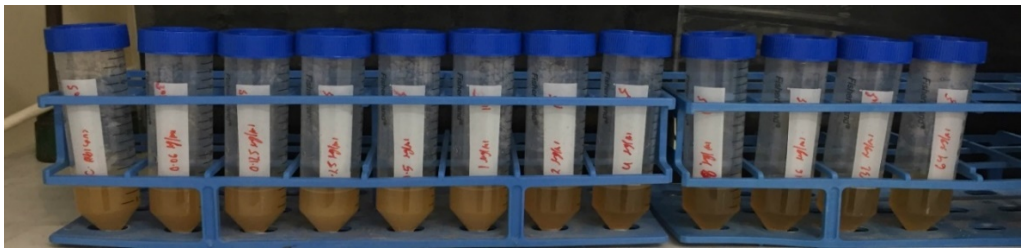

Fig. S3. MIC determination of pure FLU *C. albicans* by broth dilution assay. The photographs were captured after 24 h incubation at 30 ºC.

For local delivery of CIP and FLU, MIC was considered as target site concentration or therapeutic concentration. In our previous study (Ahmed et al., 2018), MIC of CIP for *E. coli*, *S. aureus* and *P. aeruginosa* was determined as 0.06, 0.5 and 0.125 µg/ml, respectively. In this study, MIC of FLU for *C. albicans* was recorded as 2 µg/ml. (Figures S3-S4 and Table S3). Both drugs were loaded into the dressings based on their MIC values. CIP was loaded at 50 µg/wafer and FLU was loaded at 500 µg, 1000 µg and 1500 µg per wafer, respectively. In the case of films, CIP was loaded at 50 µg per 6 mm of film sheet and FLU was loaded at 500 µg and 1000 µg per 6 mm of film sheet, respectively. CIP was loaded as 50 µg/wafer and in addition to that FLU was loaded as 500 µg, 1000 µg and 1500 µg per wafer respectively. In case of films, CIP was loaded as 50 µg/6 mm of film sheet and FLU was loaded as 500 µg and 1000 µg per 6 mm of film sheet respectively. Considering the lowest drug content, CA-CIP: FLU (1:10) films showed CIP and FLU recovery of about 32 and 445 µg/6 mm of film sheet. Broth dilution study was carried out in 10 ml media that means concentrations of drugs are 3.2 and 44.5 µg/ml for CIP and FLU respectively, which can easily meet the MIC for the studied organisms. Moreover, considering the lowest drug release from the dressings, CA-CIP: FLU (1:10) films showed CIP and FLU release of about 67.8% (21.7 µg) and 81.4% (362.2 µg) respectively. With consideration of drug release, drug concentrations are 2.2 and 36.2 µg/ml for CIP and FLU respectively which is above the MIC for the studied organisms, and therefore expected to be therapeutically active.

Table S3. CIP and FLU recoveries from the drug loading study are tabulated below.

Formulation	Theoretical content of CIP (µg)	Recovery of CIP (%)	Recovery of CIP (µg)	Theoretical content of FLU (µg)	Recovery of FLU (%)	Recovery of FLU (µg)
CA-CIP:FLU (1:10) F	50.0	64.0	32.0	500	89	445
CA-CIP:FLU (1:20) F	50.0	91.0	45.5	1000	65.6	656
CA-CIP:FLU (1:10) W	50.0	87.4	43.7	500	85.0	425
CA-CIP:FLU (1:20) W	50.0	81.1	40.6	1000	83.2	832
CA-CIP:FLU (1:30) W	50.0	81.7	40.9	1500	70.5	1057.5

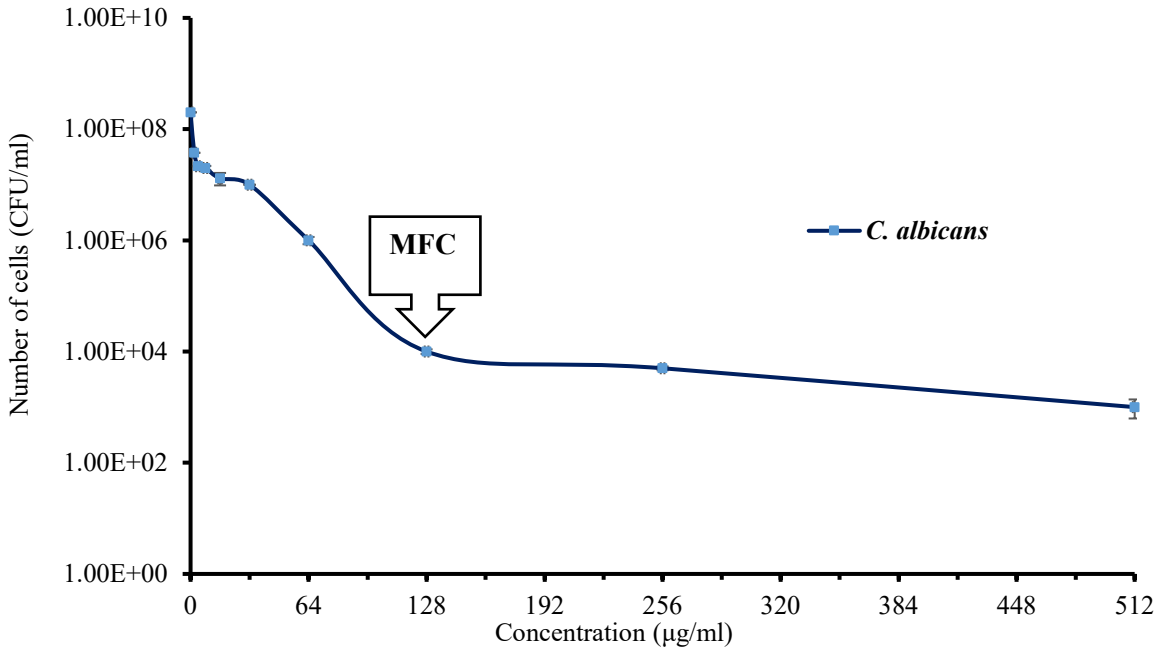

Fig. S4. Killing curve for *C. albicans* at different concentration of FLU to determine MFC (99.9% cell reduction) ($n = 3 \pm SD$).

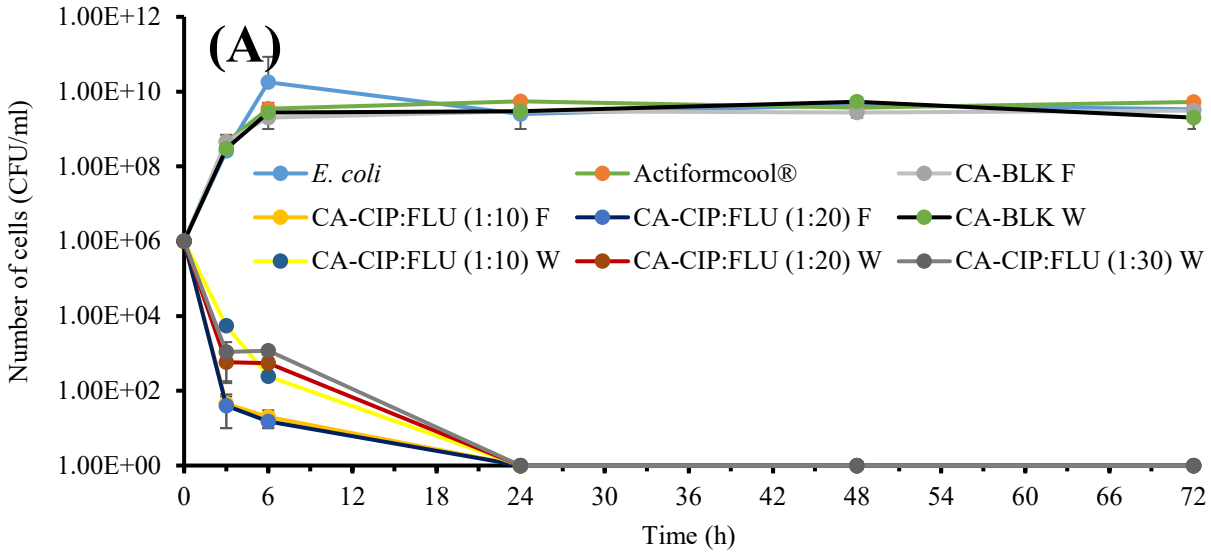
(A)
Number of cells (CFU/ml)
1.00E+12
1.00E+10
1.00E+08
1.00E+06
1.00E+04
1.00E+02
1.00E+00
0
6
12
18
24
30
36
42
48
54
60
66
72
Time (h)
E. coli
Actiformcool®
CA-BLK F
CA-CIP:FLU (1:10) F
CA-CIP:FLU (1:20) F
CA-BLK W
CA-CIP:FLU (1:10) W
CA-CIP:FLU (1:20) W
CA-CIP:FLU (1:30) W

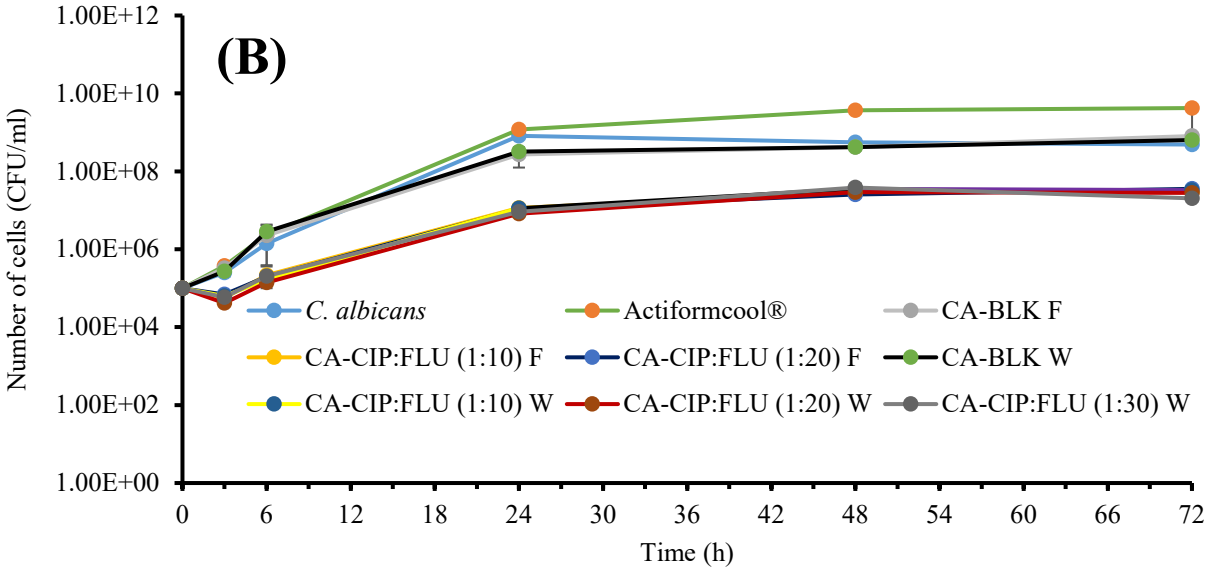
(B)
Number of cells (CFU/ml)
1.00E+12
1.00E+10
1.00E+08
1.00E+06
1.00E+04
1.00E+02
1.00E+00
0
6
12
18
24
30
36
42
48
54
60
66
72
Time (h)
C. albicans
Actiformcool®
CA-BLK F
CA-CIP:FLU (1:10) F
CA-CIP:FLU (1:20) F
CA-BLK W
CA-CIP:FLU (1:10) W
CA-CIP:FLU (1:20) W
CA-CIP:FLU (1:30) W

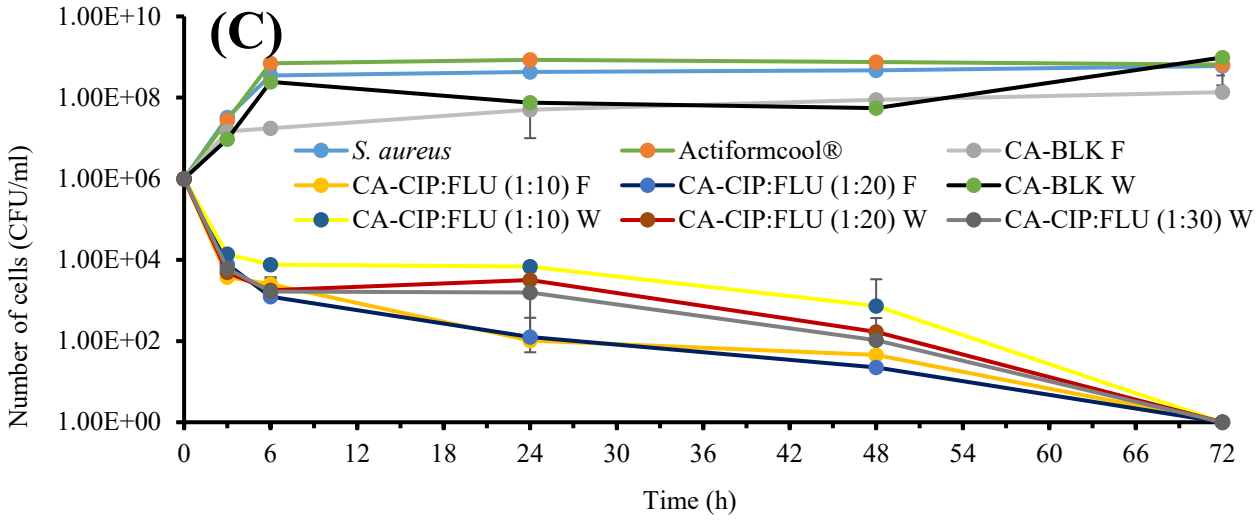
(C)
Number of cells (CFU/ml)
1.00E+10
1.00E+08
1.00E+06
1.00E+04
1.00E+02
1.00E+00
0
6
12
18
24
30
36
42
48
54
60
66
72
Time (h)
S. aureus
Actiformcool®
CA-BLK F
CA-CIP:FLU (1:10) F
CA-CIP:FLU (1:20) F
CA-BLK W
CA-CIP:FLU (1:10) W
CA-CIP:FLU (1:20) W
CA-CIP:FLU (1:30) W

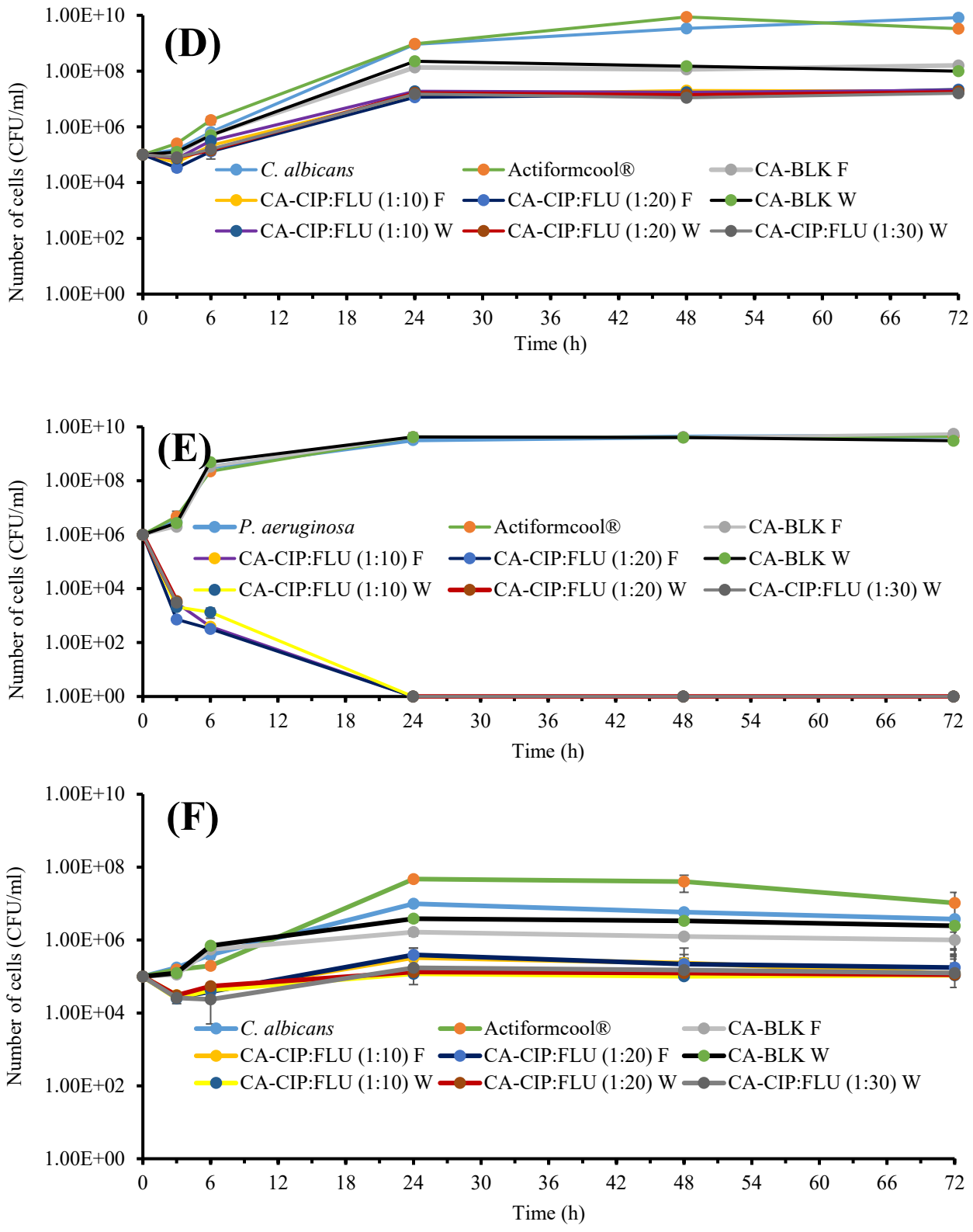

Fig. S5. Time-kill curves for combined DL dressings and Actiformcool® against the mixed infection of (A) *E. coli* and (B) *C. albicans,* (C) *S. aureus* and (D) *C. albicans,* and (E) *P. aeruginosa* and (F) *C. albicans* ($n = 3 \pm$ SD). F: Film; W: Wafer

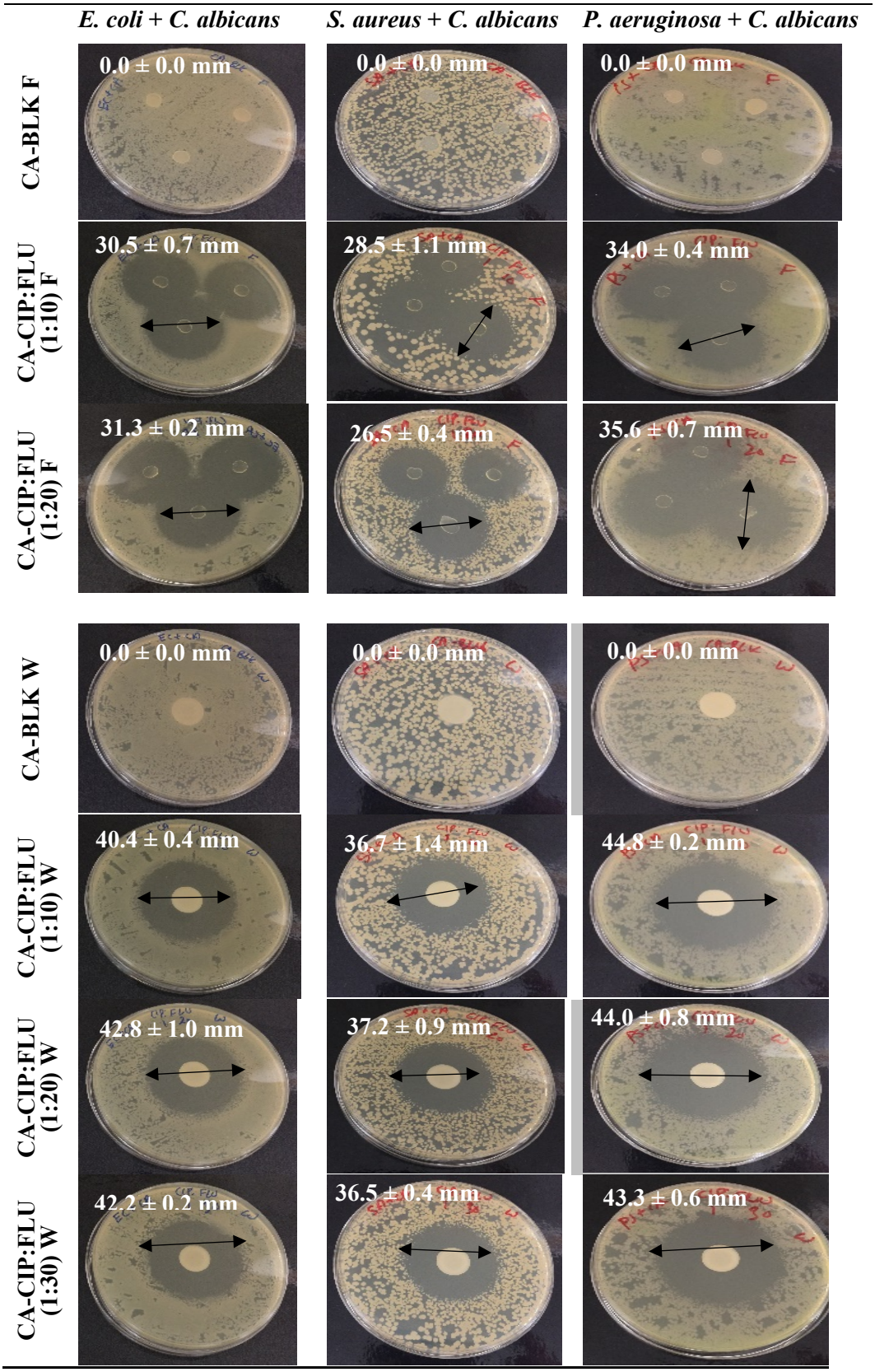

Fig. S6. Photographic images of ZOI (n = 3 ± SD) of BLK and combined DL (CIP and FLU) films and wafers against the mixed culture of bacteria (*E. coli*, *S. aureus* and *P. aeruginosa*) and fungi (*C. albicans*).

Table S4. FTIR bands of CA, CIP and FLU with peak characteristics and assignments.

Starting materials	Vibration (cm^{-1})	Peak characteristics and assignment
CA	3638 – 2941 (broad)	OH stretch
	1591	Asymmetric stretch of –COO–
	1411	Symmetric stretch of –COO–
	1025	C-O-C antisymmetric stretch of pyranosyl ring
	947	C-O stretch of uronic acid in Alginate
	874	β-C1-H deformation vibration
CIP	3600 – 3045 (broad)	OH stretch
	3000 – 2845	alkene and C-H stretch
	1675 – 1660	carbonyl C=O stretching
	1650 – 1600	quinolones
	1450 – 1400	carbonyl group (C-O) vibration
	1300 – 1250	bending vibration of O-H group
	1050 – 1000	aryl fluoride (C-F) stretching vibration
FLU	3715 – 3633	OH stretch
	2981	C-H stretch of triazole ring
	1618	C=C stretching of 2,4-difluorobenzyl group
	1500	C-C stretch of aromatic ring
	1408	$C-H_2$ scissor of propane backbone
	1270	C-F stretch of 2,4-difluorobenzyl group
	1210	β-CH stretch of triazole ring
	1135	ring breathing of triazole group
	1115	C-C stretch of propane backbone
	1075	CH deformation of 2,4-difluorobenzyl group
	1011	C-(OH) stretching of propane backbone
	960	ring bending of triazole group
	845	γ-CH triazole ring
	673	deformation of aromatic ring

Table S5. Photomicrographs (4x) showing the proliferation of human PEK cells seeded at a density of 1 x 10^5 cells/ml with the combined DL dressings. Scale bar: 500 µm.

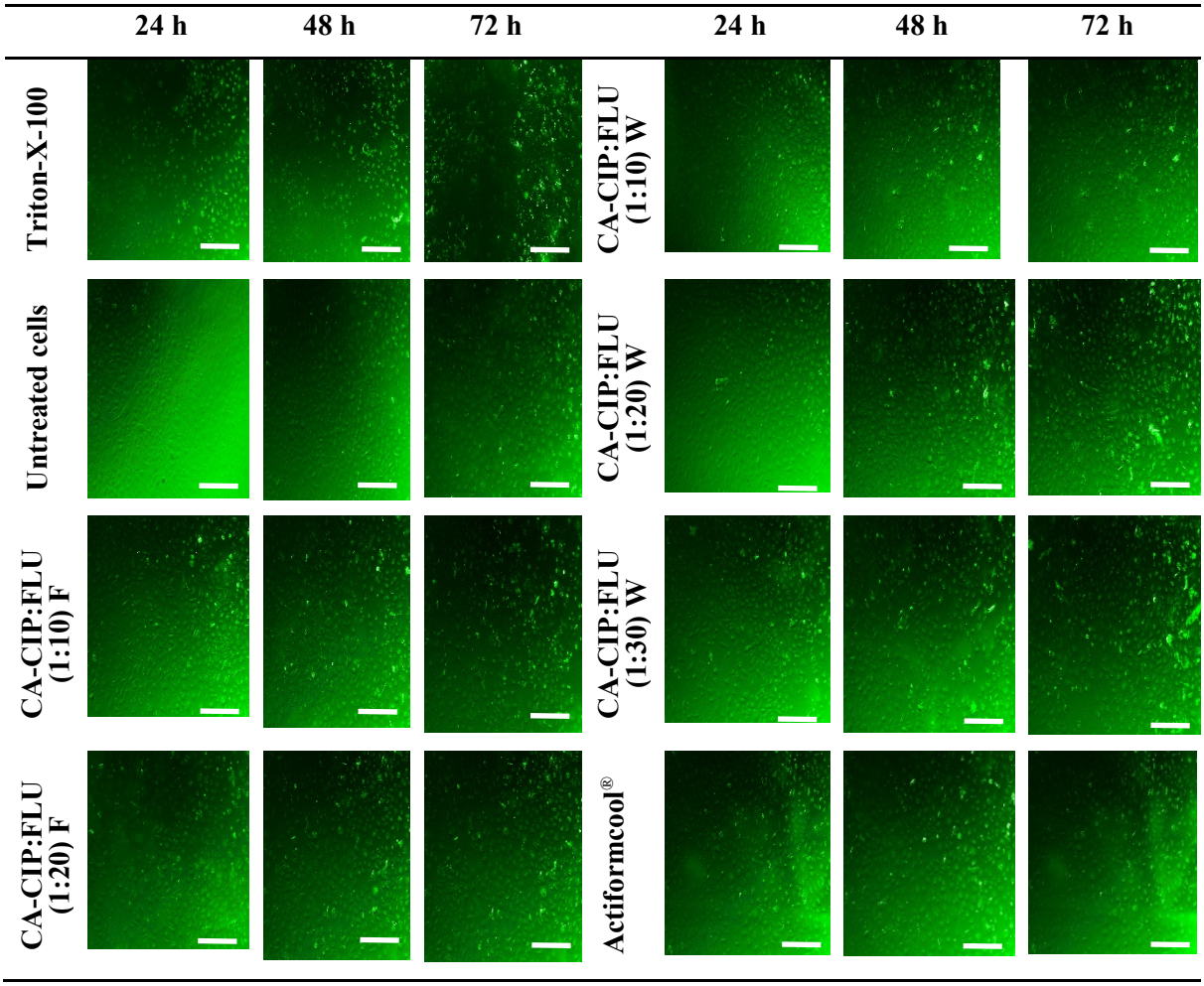

Table S6. *In vitro* wound scratch assay on human PEK cells treated with the extracts of Actiformcool®, formulated BLK and DL dressings. Triton-X-100 and untreated cells represent positive and negative controls, respectively. The blue arrows indicate wound gap (migration zone). Scale bar: 500 µm.

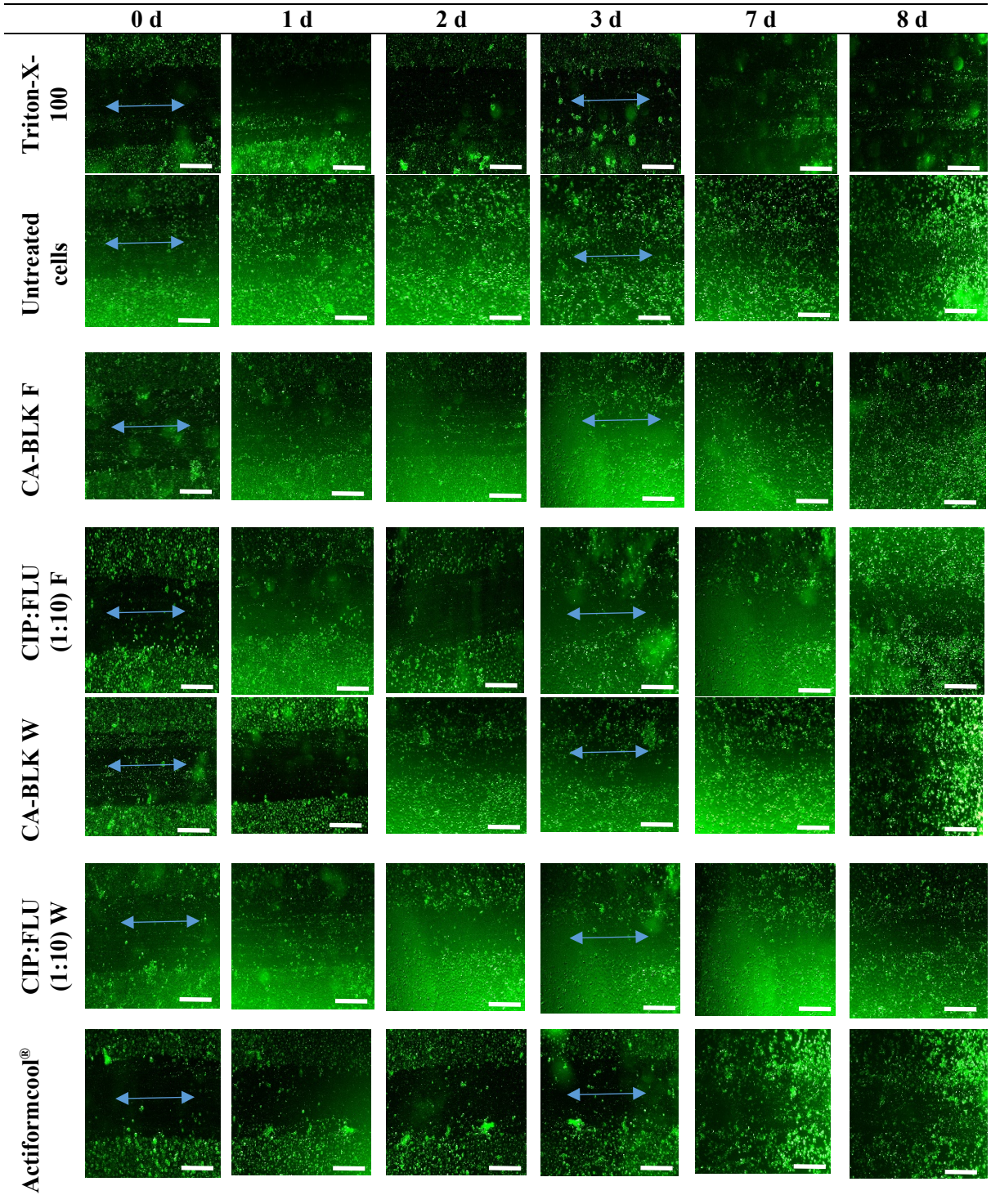

References

Ayensu, I., Mitchell, J.C., Boateng, J.S., 2012a. Development and physico-mechanical characterisation of lyophilised chitosan wafers as potential protein drug delivery systems via the buccal mucosa. Colloids Surfaces B Biointerfaces 91, 258–265. https://doi.org/10.1016/j.colsurfb.2011.11.004

Ayensu, I., Mitchell, J.C., Boateng, J.S., 2012b. In vitro characterisation of chitosan based xerogels for potential buccal delivery of proteins. Carbohydr. Polym. 89, 935–941. https://doi.org/10.1016/j.carbpol.2012.04.039

Maheronnaghsh, M., Tolouei, S., Dehghan, P., Chadeganipour, M., Yazdi, M., 2016. Identification of Candida species in patients with oral lesion undergoing chemotherapy along with minimum inhibitory concentration to fluconazole. Adv. Biomed. Res. 5. https://doi.org/10.4103/2277-9175.187394

Okoye, E.I., Okolie, T.A., 2015. Development and in vitro characterization of ciprofloxacin loaded polymeric films for wound dressing. *4*(4), 234-242. https://doi.org/10.4103/2278-344X.167660.

Topman, G., Lin, F. H., & Gefen, A. (2012). The influence of ischemic factors on the migration rates of cell types involved in cutaneous and subcutaneous pressure ulcers. *Annals of Biomedical Engineering*, *40*(9), 1929–1939. https://doi.org/10.1007/s10439-012-0545-0.

Vishal Gupta, N., Shivakumar, H.G., 2012. Investigation of Swelling Behavior and Mechanical Properties of a pH-Sensitive Superporous Hydrogel Composite. Iran. J. Pharm. Res. 11(2), 481–493. https://doi.org/10.1021/la980982.